

# Drivers of surface salinity changes in the Greenland-Iceland Seas on seasonal and interannual time scales - a climate model study

Helene Reinertsen Langehaug<sup>1</sup>, Ailin Brakstad<sup>2</sup>, Kjetil Våge<sup>2</sup>, Emil Jeansson<sup>3</sup>, Mehmet Ilicak<sup>4</sup>, and Caroline A. Katsman<sup>5</sup>

<sup>1</sup>Nansen Environmental and Remote Sensing Center

<sup>2</sup>University of Bergen

<sup>3</sup>NORCE Norwegian Research Centre, Bjerknes

<sup>4</sup>Istanbul Technical University

<sup>5</sup>Delft University of Technology

November 24, 2022

## Abstract

The Arctic climate is changing dramatically, especially in terms of sea ice loss, with potentially large downstream impacts on the Nordic Seas and the North Atlantic Ocean. The East Greenland Current (EGC) transports substantial amounts of freshwater (in liquid and solid states) southward along the east Greenland continental slope. To increase our understanding of the drivers of surface salinity changes in the interior Nordic Seas, we investigate the diversion of freshwater from the EGC into the Nordic Seas. To this end, we analyse the outcomes of an ocean model hindcast for the period 1973-2004 with a horizontal resolution of 0.25 degree. We find that sea ice contributes large amounts of freshwater to the interior Nordic Seas. On an interannual time scale, this sea ice diversion has a high and significant correlation with surface salinity in the Greenland and Iceland Seas (correlation  $< -0.7$ ). On a seasonal time scale, the model hindcast and observations demonstrate a clear signal in surface salinity: a lateral migration of the Polar Front position occurring along all of east Greenland. In the model hindcast, these lateral shifts in the front are consistent with seasonal changes in the westward wind-driven Ekman transport. Thus, this climate model study indicates that there are two main causes of seasonal and interannual surface salinity changes; wind-driven Ekman transport and sea ice diversion from the EGC, respectively.

1                                   **Drivers of surface salinity changes in the**  
2                                   **Greenland-Iceland Seas on seasonal and interannual**  
3                                   **time scales – a climate model study**

4                   **H.R. Langehaug<sup>1,2</sup>, A. Brakstad<sup>2</sup>, K. Våge<sup>2</sup>, E. Jeansson<sup>3</sup>, M. Ilıcak<sup>3,4</sup>, C.A.**  
5                                   **Katsman<sup>5</sup>**

6                   <sup>1</sup>Nansen Environmental and Remote Sensing Center, and Bjerknes Centre for Climate Research,  
7                                   Thormøhlensgate 47, 5006 Bergen, Norway

8                   <sup>2</sup>Geophysical Institute, University of Bergen and Bjerknes Centre for Climate Research, Allégaten 70,  
9                                   5007 Bergen, Norway

10                   <sup>3</sup>NORCE Norwegian Research Centre, Bjerknes Centre for Climate Research, Jahnebakken 5, 5007,  
11                                   Bergen, Norway

12                   <sup>4</sup>Eurasia Institute of Earth Sciences, Istanbul Technical University, Istanbul, Turkey

13                   <sup>5</sup>Department of Hydraulic Engineering, Delft University of Technology, Civil Engineering and  
14                                   Geosciences, Environmental Fluid Mechanics, Delft, Netherlands

15                   **Key Points:**

- 16                   • Lateral shifts in the Polar Front occur along all of east Greenland controlled largely  
17                                   by seasonal changes in the westward Ekman transport
- 18                   • 41 percent of the solid freshwater transport in Fram Strait is diverted from the  
19                                   East Greenland Current into the interior Nordic Seas
- 20                   • Interannual changes in the solid freshwater diversion is a key driver for surface salin-  
21                                   ity changes in the Greenland and Iceland Seas

---

Corresponding author: Helene Reinertsen Langehaug, [helene.langehaug@nersc.no](mailto:helene.langehaug@nersc.no)

## Abstract

The Arctic climate is changing dramatically, especially in terms of sea ice loss, with potentially large downstream impacts on the Nordic Seas and the North Atlantic Ocean. The East Greenland Current (EGC) transports substantial amounts of freshwater (in liquid and solid states) southward along the east Greenland continental slope. To increase our understanding of the drivers of surface salinity changes in the interior Nordic Seas, we investigate the diversion of freshwater from the EGC into the Nordic Seas. To this end, we analyse the outcomes of an ocean model hindcast for the period 1973-2004 with a horizontal resolution of 0.25 degree. We find that sea ice contributes large amounts of freshwater to the interior Nordic Seas. On an interannual time scale, this sea ice diversion has a high and significant correlation with surface salinity in the Greenland and Iceland Seas (correlation  $< -0.7$ ). On a seasonal time scale, the model hindcast and observations demonstrate a clear signal in surface salinity: a lateral migration of the Polar Front position occurring along all of east Greenland. In the model hindcast, these lateral shifts in the front are consistent with seasonal changes in the westward wind-driven Ekman transport. Thus, this climate model study indicates that there are two main causes of seasonal and interannual surface salinity changes; wind-driven Ekman transport and sea ice diversion from the EGC, respectively.

## Plain Language Summary

The main export pathway of freshwater from the Arctic Ocean to the North Atlantic Ocean is the East Greenland Current that flows southward along the east Greenland continental slope. The freshwater is transported both in liquid and solid (as sea ice) states. In this study, we use a global climate model to investigate freshwater diversion from the East Greenland Current and find that 41% of the sea ice export through Fram Strait melts in the interior Nordic Seas. This freshwater inflow may substantially impact where and how much dense water is formed. On an interannual time scale, the model results suggest that this sea ice diversion is an important regulator for the surface salinity across the western Nordic Seas. On a seasonal time scale, large-scale surface salinity changes in the western Nordic Seas are controlled by another process, namely wind-driven westward transport in the upper layers of the ocean.

## 1 Introduction

One of the main exits of freshwater from the Arctic Ocean is via the western part of Fram Strait, both on the shallow east Greenland shelf and via the East Greenland Current (EGC), which is tied to the shelf break (Fig. 1, e.g., Håvik et al., 2017). The freshwater is transported in the ocean either in liquid or in solid phase (as sea ice). The impact of freshwater can be substantial in key dense-water formation regions, such as the Greenland and Iceland Seas, as it may reduce the depth and density of winter convection and thereby affect the ocean circulation (e.g., Ikeda et al., 2001; Brakstad et al., 2019). The impact of freshwater on the large-scale ocean circulation has been investigated in a number of studies, especially because of the possible future weakening of the meridional overturning circulation in the Atlantic Ocean (Weijer et al., 2020) resulting from an additional freshwater input at high latitudes (e.g., IPCC, 2019; Ionita et al., 2016; Sgubin et al., 2017). However, the impact that increased freshwater input in the Nordic Seas may have on the circulation is highly dependent on *where* it is geographically distributed (Lambert et al., 2016, 2018).

In this study, we focus on mechanisms or processes that divert freshwater from the EGC into the western Nordic Seas in a climate model. Both the solid and liquid freshwater transports through Fram Strait are potential sources of freshwater in the Nordic Seas. Dodd et al. (2009) found, using tracers (salinity, oxygen isotope ratio, and dissolved barium concentration), that a significant amount (80%) of the sea ice exported through

72 Fram Strait escapes into the interior Nordic Seas. In the Labrador Sea, mechanisms by  
 73 which freshwater can be transported from the boundary current to the interior have re-  
 74 cently been investigated. There coastal upwelling winds play an important role in trans-  
 75 porting freshwater away from the coast (Schulze Chretien & Frajka-Williams, 2018; Caste-  
 76 lao et al., 2019). Here we investigate in particular the relation between variations in winds,  
 77 the associated Ekman transport and the surface salinity in the Greenland and Iceland  
 78 Seas for a relatively long time period (1973-2004). Based on observations, it has been  
 79 suggested that seasonal variability in the onshore Ekman transport in the western Ice-  
 80 land Sea regulate the location of the Polar Front, which subsequently impacts ventila-  
 81 tion in this region (Våge et al., 2018). A recent high-resolution modelling study also found  
 82 a strong relation between winds and salinity changes in the Greenland Sea, and that such  
 83 changes occur also on a shorter time scale than the seasonal cycle (Spall et al., 2021).  
 84 In the present study, we focus also on longer time scales and explore how variations in  
 85 both winds, through Ekman transport, and sea ice impact salinity variations in the Green-  
 86 land and Iceland Seas, using a 32-year long climate model simulation. With a better un-  
 87 derstanding of the mechanisms that divert freshwater into the interior Nordic Seas, we  
 88 can better predict future changes in key dense-water formation regions, and potentially  
 89 subsequent changes in the overturning circulation.

90 The solid freshwater transport through Fram Strait brings substantial amounts of  
 91 freshwater southward (e.g., Smedsrud et al., 2008). Annually, about 10% of the sea ice  
 92 area within the Arctic Basin is exported via this route; the sea ice export through the  
 93 other Arctic gateways is an order of magnitude smaller (Kwok, 2009). The ice export  
 94 is largely driven by local winds (Vinje, 2001). Exploiting the fact that there is a high  
 95 correlation between wind and sea ice area export in Fram Strait, the annual mean sea  
 96 ice area export was estimated to  $0.75 \cdot 10^6 \text{ km}^2/\text{year}$  for the period 1957-2005 using NCEP  
 97 data (Langehaug et al., 2013). In the 1990s the mean sea ice thickness in Fram Strait  
 98 was 3.4 m (Hansen et al., 2013). Using this thickness, the annual mean sea ice export  
 99 in Fram Strait is estimated as 62 mSv ( $1 \text{ mSv} = 1 \times 10^3 \text{ m}^3/\text{s}$ ) of freshwater, slightly higher  
 100 than the estimate for the period 2000-2010 (60 mSv; Haine et al., 2015). The solid fresh-  
 101 water transport through Denmark Strait is much lower than that through Fram Strait,  
 102 amounting to less than 20 mSv according to a high-resolution modelling study (Behrens  
 103 et al., 2017).

104 A substantial amount of liquid freshwater is also carried southward with the EGC.  
 105 The liquid freshwater in Fram Strait has been monitored over several decades. The long-  
 106 term annual mean is about 69 mSv (Karpouzoglou et al., 2022). Thus, the solid and liq-  
 107 uid freshwater transports are almost equal in magnitude in Fram Strait. In Denmark Strait,  
 108 the liquid freshwater transport has been estimated to 94 mSv, based on an 11-month moor-  
 109 ing record just north of the strait (de Steur et al., 2017). This showed a large variabil-  
 110 ity in the freshwater transport over the year, where values in fall were found to be higher  
 111 than 170 mSv (de Steur et al., 2017). The increase in liquid freshwater transport between  
 112 the two straits, in the downstream direction, seems to suggest that most of the liquid  
 113 freshwater transport in Fram Strait feeds into Denmark Strait. The liquid freshwater trans-  
 114 port in Denmark Strait is further strengthened by a sizeable amount of freshwater origi-  
 115 nating from sea ice melt between the two straits (Dodd et al., 2009). How much fresh-  
 116 water does reach the interior Nordic Seas? The studies above may imply that little liq-  
 117 uid freshwater from Fram Strait enters into the interior Nordic Seas. Whether this is in-  
 118 deed the case is the focus of the present study; we investigate primarily how solid fresh-  
 119 water and wind influence salinity in the Greenland and Iceland Sea. We note that ocean  
 120 currents and eddies can also bring liquid freshwater from the EGC into the interior Nordic  
 121 Seas. It has been estimated that approximately 10 mSv of freshwater flows eastward with  
 122 the Jan Mayen Current (Dickson et al., 2007), while 3.4 mSv is carried southeastward  
 123 with the East Icelandic Current (Macrandar et al., 2014). The latter value is the annual  
 124 mean over a 10-year period (2002-2012). These narrow currents and eddies, neither of  
 125 which are properly resolved by the model, are not a focus in this study, but we discuss

126 results from a high-resolution model in the Nordic Seas to better understand the exchange  
127 of liquid freshwater from the shelf to the interior (Spall et al., 2021).

128 Dense-water formation in the Greenland and Iceland Seas has been studied for a  
129 long time (e.g., Helland-Hansen and Nansen 1909, Swift & Aagaard, 1981; Karstensen  
130 et al., 2005; Våge et al., 2015; Brakstad et al., 2019). The dense water formed in the Nordic  
131 Seas is an important source to the large-scale Atlantic Meridional Overturning Circu-  
132 lation (e.g., Chafik & Rossby, 2019), as a substantial part of the dense water spilling across  
133 the Greenland-Scotland Ridge on either side of Iceland likely originates in the Green-  
134 land and Iceland Seas (e.g., Olsson et al., 2005; Jeansson et al., 2008; Eldevik et al., 2009;  
135 Mastropole et al., 2017). In this study, we are not investigating dense-water formation  
136 itself in detail. Rather, we focus on how freshwater diversion impacts changes in surface  
137 salinity in the Greenland and Iceland Sea. As Brakstad et al. (2019) showed, in this re-  
138 gion surface salinity exerts substantial influence on dense-water formation.

139 As global climate models are frequently used to explore both regional near-term  
140 climate predictions and long-term future projections in the Atlantic-Arctic region (e.g.,  
141 Weijer et al., 2020; Khosravi et al., 2022), it is important to assess how these relatively  
142 coarse-resolution models represent key features (e.g., large-scale ocean circulation, sea  
143 ice transports, wind forcing) in this region. However, the western Nordic Seas is chal-  
144 lenging to study both numerically and observationally. Numerically it is challenging be-  
145 cause of the small Rossby radius of deformation (4-5km; Nurser & Bacon, 2014), which  
146 implies that  $1/25^\circ$ -resolution model is needed to properly resolve eddy activity in the  
147 western Nordic Seas (Hallberg, 2013). In this study, we use an eddy permitting,  $1/4^\circ$ -  
148 resolution, global ocean-sea ice model with realistic atmospheric forcing for the period  
149 1973-2004. In the western Nordic Seas, this resolution (about 25 km) is not high enough  
150 to resolve the Rossby radius and associated mesoscale processes. However, the horizon-  
151 tal resolution is better than classical IPCC type climate models with resolution of  $1^\circ$   
152 in the ocean. While instabilities and eddies in the boundary current are clearly important  
153 for freshwater diversion into the interior (e.g., Spall et al., 2021), large-scale mechanisms  
154 such as wind-driven Ekman transport also matter. These can be investigated at the res-  
155 olution of climate models. Observationally, the westernmost part of the Nordic Seas is  
156 severely under-sampled (e.g., Behrendt et al., 2018) due to its harsh conditions and sea  
157 ice cover, especially during winter. Thus, it is to some extent challenging to assess the  
158 performance of models in this region. At the same time, models are needed as they can  
159 contribute to enhanced understanding of dominant processes or mechanisms. In lack of  
160 observational estimates of freshwater diversion from the EGC into the interior, we later  
161 discuss results from a recently published study, simulating the Nordic Seas for a seasonal  
162 cycle using a high-resolution regional model (2-4km; Spall et al., 2021).

163 Using the global climate model, we address seasonal and interannual variability of  
164 large-scale features in the western Nordic Seas over the 32-year long simulation. This  
165 long time span is a great advantage, as it better allows us to identify statistically sig-  
166 nificant relationships, e.g., between wind forcing and hydrography. In Section 2, we first  
167 introduce the model, secondly, we assess the horizontal distribution of large-scale cur-  
168 rents, eddy kinetic energy, and salinity in the western Nordic Seas, and finally, we de-  
169 scribe how liquid and solid freshwater fluxes are calculated. In Section 3, we first present  
170 and evaluate the simulated freshwater transports through Fram Strait and Denmark Strait,  
171 then we assess the freshwater diversion into the interior of the Nordic Seas. In Section  
172 4, we investigate the relation between wind forcing and surface salinity in the Greenland  
173 and Iceland Seas. We find that increased surface salinity in the Greenland and Iceland  
174 Seas is associated with increased westward Ekman transport in the same region, and that  
175 these fluctuations have a clear seasonal cycle. On an interannual time scale, we find that  
176 increased surface salinity in the Greenland and Iceland Seas is associated with less sea  
177 ice entering the interior Nordic Seas. Finally, we discuss the results and draw the main  
178 conclusions from this study in Section 5.

## 179 2 Model, observations, and methods

### 180 2.1 Description of the model simulation

181 We use the ocean sea-ice components of the Norwegian Earth System Model (NorESM,  
 182 Bentsen et al., 2013), where the atmospheric component is replaced with realistic inter-  
 183 annual COREv2 atmospheric forcing (Large & Yeager, 2009) for a 60-yr period (1948-  
 184 2007). Surface fluxes are calculated using the bulk formulae as described in Large & Yeager  
 185 (2004; 2009). This  $1/4^\circ$ -resolution version of NorESM has been utilized in previous  
 186 studies (Guo et al., 2016; Langehaug et al., 2019), but not the current simulation. The  
 187 main difference in this simulation compared with Langehaug et al. (2019) is that the present  
 188 simulation includes a sub-grid mesoscale eddy parameterisation.

189 NorESM was run for one cycle (i.e., 60 years) due to the costly integration of the  
 190 model. We primarily investigate the last part of the cycle, i.e., the time period 1973-2004  
 191 (model years 26-57), to avoid model drift and a salinity outlier at the end of the simu-  
 192 lation. In climate models, which integrate on longer time scales, monthly averages are  
 193 typically saved. From the simulation, we thus consider only monthly mean values.

194 The ocean component (MICOM, Miami Isopycnic Coordinate Ocean Model) in NorESM  
 195 uses an Arakawa C-grid in the horizontal and 51 density layers as the vertical coordi-  
 196 nate (Bentsen et al., 2013). For a more realistic response to atmospheric forcing, a sur-  
 197 face mixed-layer is represented by two model layers, where potential density can evolve  
 198 freely. The 51 density layers range from  $\sigma_2 = 28.202$  to  $\sigma_2 = 37.800$   $\text{kg/m}^3$  ( $\sigma_2$  is po-  
 199 tential density referenced to 2000 dbar; Bentsen et al., 2013). The mixed-layer depth in  
 200 the model is parameterised by a turbulent kinetic energy balance equation based on Oberhuber  
 201 (1993), extended with parameterised mixed-layer re-stratification according to Fox-Kemper  
 202 et al. (2008) with a coefficient of 0.06. This represents the amount of sub-mesoscale ed-  
 203 dies in a grid cell, where 0.06 is the canonical value given in Fox-Kemper et al. (2008).

204 The parameterised diapycnal mixing consists of several components: Parameterised  
 205 shear-induced mixing depends on a two-equation turbulence closure scheme (k-epsilon)  
 206 with Canuto-A stability function (Ilicak et al., 2008); a fraction of the energy extracted  
 207 from the mean flow by bottom drag drives mixing in the lowermost isopycnic layers (Legg  
 208 et al., 2006); tidal-induced mixing is parameterised according to Simmons et al. (2004);  
 209 the background mixing is latitude-dependent and vertically constant (Gregg et al., 2003),  
 210 giving a gradual decrease of diffusivity towards the equator with a value of  $105 \text{ m}^2/\text{s}$  at  
 211  $30^\circ$  latitude.

212 This configuration of NorESM uses the thickness diffusivity parameterisation com-  
 213 monly known as Gent and McWilliams (1990) to remove the available potential energy  
 214 due to unresolved mesoscale eddies. The thickness diffusivity values are computed us-  
 215 ing Eden and Greatbatch (2008). Isonutral diffusion values are set equal to thickness  
 216 diffusivity values, and they are turned off if the model resolves the Rossby radius of de-  
 217 formation locally (similar to the method described by Hallberg, 2013). NorESM also em-  
 218 ploys a biharmonic Smagorinsky viscosity operator to damp high-frequency grid noise  
 219 (Smagorinsky, 1993).

220 Sea Surface Salinity (SSS) restoring (using World Ocean Atlas climatology) is ap-  
 221 plied globally to avoid local salinity drift. The restoring is applied with a relaxation time  
 222 scale of 300 days within the first 50 meters of the water column. This value is consid-  
 223 ered mild relaxation compared to the CORE2 protocol (Danabasoglu et al., 2014). SSS  
 224 restoring is turned off if the absolute bias is larger than 0.5.

### 225 2.2 Observations

226 The salinity observations used in this study are described in (Huang et al., 2020).  
 227 In Fig. 2, we show the surface salinity in the Nordic Seas for the period 1986-2004. The

228 western Nordic Seas with the Greenland and Iceland Seas is known as the *Arctic domain*  
 229 and separates the low-salinity Polar Water to the west from the high-salinity Atlantic  
 230 Water to the east (Helland-Hansen and Nansen, 1909). The *Polar Front* separates the  
 231 Polar and Arctic water masses (Swift & Aagaard, 1981). Following Swift and Aagaard  
 232 (1981), we define the Polar Front as the 34.5 isohaline. A seasonal migration of the Po-  
 233 lar Front is clearly shown in the observations (black line; Fig. 2). In summer (Jul-Sep),  
 234 the Polar Front has its easternmost position, while the front shifts towards Greenland  
 235 in fall and winter (Oct-Mar). In spring (Apr-Jun), the front migrates back to the east.  
 236 In a recent study, Våge et al. (2018) found that the lateral extent of Polar Water varies  
 237 seasonally in the northwest Iceland Sea. They hypothesized that these lateral shifts are  
 238 linked to seasonal changes in wind forcing and Ekman transport. The observations used  
 239 herein demonstrate, for the first time, that the seasonal east-west migration of the Po-  
 240 lar Front occurs not only in the Iceland Sea but along all of east Greenland.

### 241 **2.3 Evaluation of the model simulation**

242 In terms of surface salinity, NorESM shows large variability in the western Nordic  
 243 Seas, our focus region, in contrast to the eastern Nordic Seas (Fig. 3). The variance is  
 244 particularly high in the central Greenland and Iceland Seas during summer (Jul-Sep).  
 245 The modelled surface salinity is compared with that of observations further below.

246 First, we address how the general circulation is represented in NorESM (Fig. 4a).  
 247 In the Nordic Seas the large-scale circulation is cyclonic, and the mid-depth circulation  
 248 is strongly topographically steered (Nøst & Isachsen, 2003; Voet et al., 2010). Near the  
 249 surface the EGC transports low-salinity Polar Water from the western Fram Strait to  
 250 Denmark Strait (e.g., Rudels et al., 2005; Håvik et al., 2017). On the opposite side of  
 251 the Nordic Seas, the Norwegian Atlantic Current and the West Spitsbergen Current trans-  
 252 port saline Atlantic Water northwards (e.g., Mauritzen, 1996; Koszalka et al., 2011).

253 The EGC is clearly evident in NorESM with its high velocities mostly along the  
 254 Greenland shelf break (Fig. 4a). Along the 1200m isobath, the simulated mixed-layer  
 255 velocity is about 15-20cm/s. This is lower than what observations indicate (e.g., Håvik  
 256 et al. (2017) found the EGC to have a core speed between 20-40cm/s). In NorESM, south  
 257 of about 75°N, the highest velocities are seen on the Greenland shelf (Fig. 4a), which  
 258 is contrary to observations, where the velocities peak along the continental shelf break  
 259 (e.g., Håvik et al., 2017). These differences may be a manifestation of limited horizon-  
 260 tal resolution of the model. Note that the model data are long-term averages over the  
 261 period 1973-2004. However, the representation of the EGC in a 1/4°-resolution (eddy-  
 262 permitting) global ocean simulation is improved over a 1°-resolution, with a stronger and  
 263 narrower EGC in the higher resolution version (Marsh et al. (2010); using NEMO, Langehaug  
 264 et al. (2019); using NorESM).

265 Secondly, we assess the eddy kinetic energy (EKE) in the model (Fig. 4b). EKE  
 266 is the kinetic energy of the time-varying component of the velocity field, and thus rep-  
 267 represents a range of processes from mesoscale to large-scale motions (Martínez-Moreno et  
 268 al., 2019). As described earlier, the horizontal resolution of NorESM is not high enough  
 269 to resolve the Rossby radius and associated mesoscale processes in the western Nordic  
 270 Seas. The EKE from the model therefore likely represents mainly the time-varying com-  
 271 ponent of the large-scale motions. The EKE is often calculated based on sea surface height,  
 272 but to use sea surface height from satellite data is difficult in the western Nordic Seas  
 273 due to sea ice (Trodahl & Isachsen, 2018). We therefore compare eddy kinetic energy  
 274 (EKE) in NorESM with that in a higher resolution model (4 km horizontal resolution;  
 275 Trodahl & Isachsen, 2018). We define EKE, as in Trodahl & Isachsen (2018):  $EKE =$   
 276  $0.5*(u'^2+v'^2)^{0.5}$ . In Fig. 4b, we show the simulated EKE calculated from mixed-layer  
 277 velocities. The simulated EKE uses  $u'$  and  $v'$  that are monthly velocity anomalies with  
 278 respect to annual mean velocities. Only monthly velocities are available from the model

279 to calculate EKE. As a consequence, the EKE that we present here is expected to be lower  
 280 than if we were to use daily velocities from the model. The simulated pattern of EKE  
 281 resembles the pattern of EKE based on the 4 km resolution model in Trodahl & Isach-  
 282 sen (2018; their Fig. 2). The highest values in NorESM (around 0.1 m/s) are found be-  
 283 tween Greenland and Iceland. EKE is also relatively high along the EGC (around 0.05  
 284 m/s) and then decreases towards the interior Nordic Seas. However, EKE in our sim-  
 285 ulation is reduced by a factor of about 2 compared to the higher resolution model. The  
 286 underestimation of EKE is likely the result of using monthly values and due to the hor-  
 287 izontal resolution of the model.

288 Thirdly, we provide a detailed examination of the salinity differences between NorESM  
 289 and the observations (Fig. 5). The simulated east-west gradient across the western Nordic  
 290 Seas differs substantially from the observations, especially during summer (Jul-Sep; Fig.  
 291 5). The largest difference between the model and the observations is on the Greenland  
 292 shelf between Fram Strait and Denmark Strait, with NorESM being too saline (salin-  
 293 ity differences of up to 2 in some locations). In winter (Jan-Mar; Fig. 5), the shelf is ice-  
 294 covered and it is difficult to observe salinity. In the interior Nordic Seas, the simulated  
 295 salinity agrees much better with the observations. Only in the Iceland Sea and the north-  
 296 ern Greenland Sea is the simulated salinity lower by up to 0.8-1 in summer. These dif-  
 297 ferences between the simulated and observed salinities are consistent with a previous study,  
 298 comparing a range of different CORE forced ocean models (including NorESM) in the  
 299 Nordic Seas and Arctic Ocean (Ilıcak et al., 2016), that all have low horizontal resolu-  
 300 tion (typically  $1^\circ \times 1^\circ$ ). Both the magnitude and the pattern of the model differences  
 301 that were found is similar to what is seen in Fig. 5, with a generally too saline Green-  
 302 land shelf, too fresh Nordic Seas interior, and too saline Atlantic Water in the east. This  
 303 suggests that the typical biases that exist in coarse-resolution models persist in the  $1/4^\circ$ -  
 304 resolution model used here.

305 Lastly, we compare the simulated Polar Front with that of observations. Because  
 306 of the salinity differences of about 0.2 along the continental slope between the model sim-  
 307 ulation and observations, it is more appropriate to choose the 34.3 isohaline than 34.5  
 308 to mark the Polar Front in the model (solid magenta line; Fig. 2). A seasonal migration  
 309 of the Polar Front is simulated in NorESM. In summer, the Polar Front has its eastern-  
 310 most position, while the front shifts towards Greenland in fall and winter. In spring, the  
 311 front migrates back to the east. The position of the front in the model is not fully aligned  
 312 with that of observations, but shows overall a similar seasonal migration (compare the  
 313 solid magenta and black lines; Fig. 2).

314 In this study, we are interested in the liquid freshwater diversion from the EGC to  
 315 the interior Nordic Seas. However, we have seen that the east-west salinity gradient in  
 316 the model differs substantially from the observed gradient. This might be related to the  
 317 limited ability of the model to properly represent eddies and ocean currents. At the same  
 318 time, there are too few observations to provide a reliable quantitative estimate of the liq-  
 319 uid freshwater entering the interior. For comparison with our model simulation, we there-  
 320 fore discuss results from a very high-resolution regional model (2-4km; Spall et al., 2021).  
 321 The Nordic Seas was simulated for one seasonal cycle from 2017-2018. Using daily mean  
 322 values, they investigated the exchange of salt and heat between the shelf and the inter-  
 323 rior of the Greenland Sea. More specifically, they quantified how oceanic advection changes  
 324 the properties of the Greenland Sea basin. Considering the annual mean, they found a  
 325 small impact along the western boundary of the Greenland Sea basin due to shelf-interior  
 326 exchange. However, on seasonal time scales they found that oceanic advection has a large  
 327 impact; increasing the salinity in winter and reducing the salinity in summer. The NorESM  
 328 results are consistent with this; increased surface salinity in the Greenland Sea during  
 329 winter is associated with increased westward Ekman transport, and reduced surface salin-  
 330 ity in summer is associated with reduced westward Ekman transport. This will be shown  
 331 in Section 3. Spall et al. (2021) further decomposed the small annual mean oceanic ad-

vection along the western boundary into mean advection and eddy advection. The mean advection was larger than the eddy advection and the two components worked in different directions; the mean advection acted to increase the salinity, whereas the eddy advection acted to decrease it. So, in summary, Spall et al. (2021) showed that seasonal exchanges between the shelf and the interior are large and related to the wind stress, whereas the annual mean exchanges are small. We will come back to this when describing the results from NorESM, considering both seasonal and interannual time scales (see Section 3).

Regarding the liquid freshwater transport in Fram Strait and Denmark Strait, we compare NorESM against estimates based on available observations. We find that the model underestimates the liquid freshwater transports in both of these straits (see Section 3).

#### 2.4 Calculation of the combined liquid and solid freshwater transports

In this study we have chosen to use freshwater transports for two practical purposes: 1) we combine the solid and liquid freshwater transports to look at the total impact of freshwater on the surface conditions in the Greenland and Iceland Seas, and, 2) we compare the liquid freshwater transport in the model with the observed liquid freshwater transport in Fram Strait and Denmark Strait (de Steur et al., 2009, 2017, 2018; Karpouzoglou et al., 2022). Currently, freshwater transports is a topic of debate. It is argued that salinity transports, without the need of a salinity reference value, would give results that is comparable from one study to another. Schauer and Losch (2019) have therefore questioned whether freshwater is useful in understanding changes in the ocean. However, when applying a model, we can check for mass balance in the targeted region to ensure that the budget is closed.

We consider the budget of the total (liquid + solid) freshwater transport (FWT) across the boundaries of the enclosed area (see Section 3), where mass is conserved within. To calculate the liquid freshwater transport, we use a similar definition and the same reference value (34.9) as de Steur et al. (2018). The solid freshwater transport is the sea ice volume transport converted to liquid freshwater transport. More details on the calculations of the freshwater transports are given in the Appendix. In the following, liquid freshwater transport refers to freshwater transport in the ocean, and solid freshwater transport refers to transport of sea ice.

#### 2.5 Sections and budget calculations

We have defined four sections that enclose the EGC (Fig. 1). The sections in Fram Strait and Denmark Strait have similar locations to the moored arrays used by de Steur et al. (2017, 2018). To capture the freshwater diversion into the interior Nordic Seas, we have defined a section that is outside the core of the EGC. The section is located along the base of the Greenland continental slope from Fram Strait to Denmark Strait (defined by mean velocities between 7 and 11 cm/s at locations deeper than 1200m; see Fig. 4a). This section is referred to as the outer EGC section. It ends in the Iceland Sea where the 1200m isobath makes a sharp turn toward the west, just north of the Spar Fracture Zone, which bisects the Kolbeinsey Ridge. The location of the Iceland section is chosen to enclose the region. All sections are aligned with the model grid cells.

The mass transport through Fram Strait is mainly balanced by the combined mass transports through the outer EGC section and Denmark Strait. The mass transport through the Iceland section is very small.

### 3 Assessing freshwater transport in the western Nordic Seas

In this section, we address the long-term mean and seasonal cycle of the simulated freshwater diversion into the interior Nordic Seas. We compare the long-term mean and seasonal FWT in Fram Strait and Denmark Strait in NorESM with observations.

#### 3.1 Long-term mean freshwater budget

We quantify the total freshwater (liquid + solid) diversion into the interior in NorESM as described in Section 2.3 (across the outer EGC section; Fig. 6). The long-term annual mean for the time period 1973-2004 is 17 mSv out of the domain. The solid freshwater diversion (19 mSv) amounts to 41% of the solid freshwater transport entering through Fram Strait (46.2 mSv). Interestingly, all of the freshwater diverted from the EGC into the interior in the model is sea ice, while the liquid part has a small negative contribution (Fig. 6). This supports the findings of Dodd et al. (2009), that sea ice is the main source of freshwater to the interior Nordic Seas. The NorESM results are also consistent with Spall et al. (2021) for the Greenland Sea, showing that the annual mean exchanges of salt between the shelf and the interior are small (a more detailed description of their results are given in Section 2.2). Across the Iceland section, there is only a small liquid freshwater transport of 1 mSv out of the domain (Fig. 6), into the southern Iceland Sea. The freshwater transport across this section therefore plays a minor role in the overall EGC freshwater budget for this model and is not further discussed.

In NorESM, the solid freshwater transport across Fram Strait is much larger than the liquid component (46.2 mSv compared to 10.3 mSv; Fig. 6). In Denmark Strait, the size of the two components are more comparable (20.1 mSv and 18.6 mSv, respectively; Fig. 6). The liquid freshwater transports across Fram and Denmark Straits have previously been quantified based on observations, and amounts to 70 mSv and 94 mSv (more details are provided in the following paragraphs; Table 1), respectively (de Steur et al., 2017, 2018). Although the model underestimates the long-term annual mean of the liquid freshwater transport, the underestimation is of similar magnitude in the two straits. The low values are likely due to the positive salinity bias in the model (too saline water on the Greenland shelf; Fig. 5). An underestimation of liquid freshwater transport in Fram Strait also appears to be a challenge in ocean reanalyses (both 1 degree and 0.25 degree resolution) and also for a finer scale model with 18km resolution (Fuentes-Franco & Koenigk, 2019; Condron et al., 2009).

The observation-based liquid freshwater transport in Fram Strait has been estimated from velocity and hydrography since 1997 (de Steur et al., 2009). The long-term annual mean liquid freshwater transport for the time period 1998-2008 is about 34 mSv (with a reference salinity of 34.8, de Steur et al., 2009), but this value does not include the liquid freshwater transport on the shelf. de Steur et al. (2009) include the shelf (with use of modelling) in their estimate, yielding 62 mSv for the total liquid freshwater transport. More recent estimates covering the period 2003 to 2015, which include the shelf, give a similar annual mean of about 64 mSv (de Steur et al., 2018). With a reference salinity of 34.9, this gives a value of 70 mSv (Table 1). A recent update gives a value of 68.6 mSv for the period 2003-2019 (Karpouzoglou et al., 2022).

North of Denmark Strait, the observation-based liquid freshwater transport was estimated based on moored velocity and hydrographic measurements from September 2011 to July 2012 (de Steur et al., 2017). The mean over that period was estimated to 94 mSv, which includes a contribution from the shelf of about 20 mSv (Table 1). The liquid freshwater transport in Denmark Strait could have been even larger, as November 2011 was a particularly anomalous month. The observational data indicate that a large eddy passed through the mooring array, which caused a temporary reversal of the flow, and therefore gave a relatively low liquid freshwater transport (de Steur et al., 2017).

428 In NorESM, the long-term annual mean solid freshwater transport in Fram Strait  
 429 (46.2 mSv) is also underestimated, but to a much lesser extent than the liquid compo-  
 430 nent. Observational studies find that the solid freshwater transport is expected to be of  
 431 comparable size to the liquid freshwater transport (Dodd et al., 2009), amounting to about  
 432 1900 km<sup>3</sup>/year or 60 mSv, where the latter is the equivalent freshwater volume stored  
 433 in sea ice between 2000 and 2010 using a reference salinity of 34.8 (Haine et al., 2015).

434 On the other hand, the solid freshwater transport in Denmark Strait (20.1 mSv)  
 435 may be somewhat overestimated in NorESM. Because we do not have observation-based  
 436 estimates of the solid freshwater transport in this region, we compare NorESM with re-  
 437 sults from a higher resolution model (1/20°, Behrens et al., 2017). This model shows sim-  
 438 ilar results as NorESM in Denmark Strait: both models have a total (liquid + solid) fresh-  
 439 water transport of about 39 mSv and both models underestimate the liquid freshwater  
 440 transport. The reason for the underestimation in the higher resolution model is likely  
 441 of same origin as in NorESM; a positive salinity bias in the Nordic Seas (Fig. 5). In a  
 442 more detailed comparison, we find that NorESM has a solid component that contributes  
 443 with 52% of the total freshwater transport (Fig. 6; averaged over 1973-2004), whereas  
 444 Behrens et al. (2017) show that the solid component contributes with 43% of the total  
 445 freshwater transport (averaged over 1960-2009). Based on this comparison, the solid fresh-  
 446 water transport in NorESM may be somewhat overestimated.

447 A similar amount of sea ice that exits Denmark Strait finds its way into the inte-  
 448 rior Nordic Seas (19 mSv; Fig. 6). Due to model biases and scarce observations, it is dif-  
 449 ficult to assess if this value is realistic. However, as the solid freshwater transports in Fram  
 450 Strait and Denmark Strait are fairly realistic, we further quantify the solid freshwater  
 451 diversion into the interior in NorESM. To determine where freshwater diverges into the  
 452 interior, the latitudinal distribution of both the liquid and solid components are shown  
 453 in Fig. 7. The freshwater diversion has been integrated into bins with a width of one de-  
 454 gree of latitude. We find that most of the solid component goes into the Greenland Sea  
 455 with a peak contribution in the southern part, at 73-74°N, (close to 7 mSv). At the same  
 456 latitude, the liquid freshwater component is less than 1 mSv. In the northern Iceland Sea  
 457 (at 70-72°N), both the solid and liquid components are negative (both components are  
 458 less than 2 mSv). The results from Fig. 7 seem to partly reflect the large-scale circula-  
 459 tion in the Greenland and Iceland Seas in NorESM. In the southern Greenland Sea, the  
 460 upper ocean circulation in NorESM shows relatively weak currents (compared to the EGC)  
 461 towards the east or southeastward (Fig. 4a). This is consistent with the location of the  
 462 peak freshwater diversion into the Greenland Sea. Close to Jan Mayen, the upper ocean  
 463 circulation shows typically a stronger westward component compared to further north  
 464 (Fig. 4a), consistent with the the total freshwater amount that is negative.

### 465 3.2 Seasonal mean freshwater budget

466 Regarding the liquid freshwater transport in Fram Strait, NorESM shows highest  
 467 values in fall (maximum in October) and lowest in spring and summer (minimum in July),  
 468 indicated by the magenta curve in Fig. 8a. This compares well with the seasonal cycle  
 469 in the observations; de Steur et al. (2018) find that the liquid freshwater transport is high-  
 470 est in late fall (November) and lowest during summer (August). North of Denmark Strait,  
 471 we also find the timing in the simulated seasonal cycle to be fairly realistic. The high-  
 472 est liquid freshwater transport in NorESM occurs in late fall (October and November;  
 473 Fig. 8b; magenta curve). After this, the liquid freshwater transport is gradually reduced  
 474 to almost zero in July. In the observations (de Steur et al., 2017), the highest liquid fresh-  
 475 water transport occurs somewhat earlier; in September and October, which is then fol-  
 476 lowed by a clear reduction from December to July. We emphasize that the NorESM re-  
 477 sults are averaged over a long time period (32 years; 1973-2004), in contrast to the ob-  
 478 servational data that were obtained over less than one year (Sep 2011-July 2012). Thus,  
 479 differences in the timing of the seasonal cycle are expected, as a single seasonal cycle might

480 differ from one year to another. We find that NorESM has large interannual variability  
 481 in the seasonal cycle of the freshwater transport (grey error bars; Fig. 8b). In Table 1,  
 482 we have listed observational studies that estimate liquid freshwater transport. Note that  
 483 several of these have taken place during summer, likely before the timing of the max-  
 484 imum liquid freshwater transport.

485 In terms of the solid freshwater transport, the seasonal cycle in NorESM is also fairly  
 486 realistic. In Fram Strait, we compare the solid freshwater transport in NorESM with observa-  
 487 tion-based sea ice volume transport shown in Zamani et al. (2019) (the solid freshwater trans-  
 488 port is dependent on the sea ice volume transport; see the Appendix). We find that the  
 489 simulated and observation-based seasonal cycles are fairly similar; the highest solid fresh-  
 490 water transport occurs in winter (Dec-Apr) and the lowest in summer (Jun-Aug; light  
 491 blue curve in Fig. 8a), same as in Zamani et al. (2019). In Denmark Strait, the seasonal  
 492 cycle of solid freshwater in NorESM compares fairly well with that shown in Behrens et  
 493 al. (2017). The highest solid freshwater transport occurs during winter and the lowest  
 494 during summer (with values close to zero; light blue curve in Fig. 8b).

495 We further investigate the seasonal cycle of the freshwater diversion into the in-  
 496 terior in a similar way as for Fram Strait and Denmark Strait (Fig. 8c). Considering only  
 497 the uppermost part of the ocean (the mixed-layer; strongly influenced by winds), we find  
 498 that the liquid freshwater diversion has a seasonal cycle (red dashed line; Fig. 8c). This  
 499 is further discussed in the following section. The seasonal cycle of the solid freshwater  
 500 diversion into the interior has a similar structure to that in Fram Strait and Denmark  
 501 Strait, with highest values during winter and lowest during summer (light blue curve;  
 502 Fig. 8c). In both the outer EGC section and Denmark Strait, the solid freshwater part  
 503 is also low during fall (Sep-Oct; Fig. 8b and 8c). Furthermore, the results display sub-  
 504 stantial interannual variability of the freshwater diversion into the interior, both for the  
 505 total and solid freshwater diversion (grey and light blue vertical lines, respectively, Fig.  
 506 8c).

507 In summary, we find in NorESM that a substantial amount of solid freshwater is  
 508 diverted into the interior Nordic Sea. We also find that the simulated seasonal cycles of  
 509 both the liquid and solid components in Fram Strait and Denmark Strait are fairly well  
 510 represented. In the following section, we further explore the seasonal variability of SSS  
 511 in the western Nordic Seas and the interannual variability of the solid freshwater diver-  
 512 sion into the interior.

## 513 4 Mechanisms controlling freshwater diversion in the western Nordic 514 Seas

515 In this section, we first investigate if there is a link between the seasonal variabil-  
 516 ity of SSS and the large-scale wind stress in the western Nordic Seas in NorESM. The  
 517 basis for this investigation is the observation-based study by Våge et al. (2018), who hy-  
 518 pothesized that there is a link between the two in the Iceland Sea. Secondly, we exam-  
 519 ine the interannual relationship between SSS in the western Nordic Seas and the fresh-  
 520 water diversion into the interior in NorESM.

### 521 4.1 Seasonal relationship between surface salinity and wind stress

522 Hydrographic observations demonstrate that the Polar Front migrates laterally on  
 523 seasonal time scales (black lines in Fig. 2). NorESM simulates a similar seasonal shift  
 524 in the location of the Polar Front (magenta lines in Fig. 2). It has been hypothesized  
 525 that these lateral shifts are linked to seasonal changes in the Ekman transport (Våge et  
 526 al., 2018). In Fig. 9, we show the Ekman transport distance in NorESM, decomposed  
 527 to its zonal and meridional components in winter (Jan-Mar). The Ekman transport dis-  
 528 tance is estimated as in Våge et al. (2018), and is defined as follows:  $X_E = \frac{\tau}{\rho f h}$ , where

529  $\tau$  is the monthly mean wind stress,  $\rho = 1025\text{kg/m}^3$  is the reference density of sea wa-  
 530 ter,  $f$  is the coriolis parameter, and  $h$  is the depth of the Ekman layer (we assume a depth  
 531 of 50m, same as in Våge et al. (2018)). All variables, except the wind stress, are con-  
 532 stants, and the Ekman transport distance is thus proportional to the wind stress. The  
 533 zonal component of the wind stress results in a substantial westward Ekman transport  
 534 during winter (Fig. 9a), while the meridional component of the wind stress gives a large  
 535 southward Ekman transport in the northern part of the Greenland Sea (Fig. 9b). Over-  
 536 all, NorESM shows that the westward Ekman transport is dominating the western Nordic  
 537 Seas in winter.

538 We consider only the western Nordic Seas (defined by the box in Fig. 9a) and in-  
 539 vestigate the link between the Ekman transport distance and SSS. The zonal Ekman trans-  
 540 port distance displays pronounced seasonal variability (black curve; Fig. 10a). The vari-  
 541 ability in the meridional component of the Ekman transport distance is much smaller  
 542 (magenta curve; Fig. 10a). The zonal component shows that the Ekman transport is west-  
 543 ward during the whole year. It is highest during winter (Jan-Mar) and fall (Oct-Dec),  
 544 and has its minimum in summer (Jul). The seasonal cycle in the zonal Ekman transport  
 545 distance is strongly correlated to SSS; SSS shows a similar cycle, but delayed by one month  
 546 (red curve; Fig. 10a).

547 A cross-correlation, using all monthly data for the period 1973-2004, confirms a sta-  
 548 tistically significant relationship at one month lag between westward Ekman transport  
 549 distance and SSS in the western Nordic Seas (black curve; Fig. 10b). Hence, a large west-  
 550 ward Ekman transport distance during winter and fall contributes to higher SSS in the  
 551 western Nordic Seas. And vice versa, a small westward Ekman transport distance dur-  
 552 ing summer contributes to lower SSS. The southward Ekman transport distance shows  
 553 a weak and non-significant correlation with SSS.

554 The NorESM results support the hypothesis of Våge et al. (2018); that the sea-  
 555 sonal migration of the Polar Front is linked to the westward Ekman transport. During  
 556 summer (Jul-Sep) the Polar Front is at its easternmost position with weak northerly winds.  
 557 As the northerly winds intensify in fall and winter, the front and the Polar Water are  
 558 pushed towards Greenland, and the front is at its westernmost position during winter  
 559 (Jan-Mar). As the winds relax during spring, the Polar Front moves eastward. As a con-  
 560 sequence, SSS in the western Nordic Seas has a pronounced wind-driven seasonality.

## 561 4.2 Interannual relationship between surface salinity and freshwater di- 562 version

563 Analysis of the total freshwater budget in NorESM over the period 1973-2004 demon-  
 564 strates a general diversion of freshwater into the interior Nordic Seas, but that there are  
 565 large fluctuations in the annual mean from year to year (black bars; Fig. 11a). The changes  
 566 in the liquid freshwater component can be of similar magnitude as in the solid freshwa-  
 567 ter component, and hence, can contribute to changes in the total freshwater diversion  
 568 (magenta and light blue curves; Fig. 11a). Considering only the uppermost layer (i.e.,  
 569 Polar Surface Water with salinity  $< 34.4$ ), we find similar changes in the liquid fresh-  
 570 water diversion (dashed line; Fig. 11a). This contribution from the liquid component is  
 571 different from the seasonal cycle in NorESM, where the total freshwater diversion was  
 572 clearly dominated by the solid freshwater component (Fig. 8c). In addition, we find that  
 573 the solid component is always positive, whereas the liquid component changes sign from  
 574 year to year. When there is a high negative peak in the liquid component (years 1984  
 575 and 2000), the total freshwater transport is also negative (i.e., there is a freshwater trans-  
 576 port directed towards Greenland). Although the changes in the solid and liquid compo-  
 577 nents can be of similar magnitude, the overall contribution to the total freshwater di-  
 578 version comes from the solid component. In the following, we address the impact of the  
 579 solid component on SSS in the western Nordic Seas in NorESM.

580 In NorESM, the temporal evolution of the solid freshwater diversion into the in-  
 581 terior appears to be anti-correlated with SSS in the western Nordic Seas (Fig. 11b); a  
 582 large diversion of solid freshwater coincides with low SSS. A cross-correlation between  
 583 the two variables confirms a statistically significant link between solid freshwater diver-  
 584 sion and SSS on interannual time scales for the period 1973-2004 (blue curve; Fig. 12).  
 585 We furthermore find that the solid freshwater diversion is positively and significantly cor-  
 586 related with the southward Ekman transport distance in the western Nordic Seas (grey  
 587 curve; Fig. 12). The main portion of the solid freshwater diversion enters into the Green-  
 588 land Sea (light blue curve; Fig. 7) during winter (light blue curve; Fig. 8c). The south-  
 589 ward Ekman transport distance is also highest during winter (magenta curve; Fig. 10a)  
 590 and the highest values are found in the northwestern Greenland Sea (Fig. 9b). This sug-  
 591 gests that the interannual variability of the solid freshwater diversion is linked in par-  
 592 ticular to the southward Ekman transport distance in the region where the EGC flows  
 593 (along the shelfbreak in the northwestern Greenland Sea).

594 To investigate the link between the freshwater diversion into the interior and SSS  
 595 in the western Nordic Seas in more detail, we use a composite analysis technique. We  
 596 assess only years related to high or low freshwater diversion, i.e., values above (below)  
 597 half of the standard deviation (Fig. 13). We find 12 years with high freshwater diver-  
 598 sion into the interior (blue circles, Fig. 13) and 10 years with either low freshwater di-  
 599 version or negative freshwater transport (red circles, Fig. 13). Note that we consider the  
 600 total freshwater transport (same as the black bars, Fig. 11a), as we investigate the com-  
 601 bined effects of liquid and solid freshwater on the spatial distribution of SSS. Compar-  
 602 ing the latitudinal distribution of total freshwater transport for high and low cases, we  
 603 find the largest differences in the freshwater diversion occurring in the Greenland Sea  
 604 (thin grey curves; Fig. 7). In addition, we find relatively large differences close to Jan  
 605 Mayen, where the total freshwater transport is typically negative.

606 In NorESM, we find that these large fluctuations in high and low freshwater trans-  
 607 ports are related to SSS anomalies in a relatively large region across the western Nordic  
 608 Seas (Fig. 14a and 14b). A high freshwater diversion corresponds to a fresh anomaly in  
 609 the western Nordic Seas (Fig. 14a). In the opposite case, when the total freshwater di-  
 610 version is low, the surface of the western Nordic Seas is more saline (Fig. 14b). We show  
 611 the SSS anomalies in late summer (Jul-Sep), as this season has the highest interannual  
 612 variability of SSS (Fig. 3). The magnitudes of the anomalies are about half of the stan-  
 613 dard deviation of SSS (compare Fig. 3 and Fig. 14a/14b). Using annual mean SSS in  
 614 the composite analysis instead of summer SSS shows a similar pattern as in Fig. 14, but  
 615 with weaker anomalies.

616 NorESM demonstrates how freshwater diversion into the interior affects SSS in a  
 617 region covering most of the western Nordic Seas. The clear relationship between high/low  
 618 freshwater diversion, especially for the solid component, and fresher/more saline surface  
 619 water in the western Nordic Seas, suggests that solid freshwater diversion is a key driver  
 620 for salinity changes in the Greenland and Iceland Seas.

## 621 5 Discussion and Conclusions

622 In this study, we have focused on drivers or mechanisms for surface salinity changes  
 623 in the western Nordic Seas; the Greenland and Iceland Seas that are influenced by a ma-  
 624 jor outflow from the Arctic Ocean (Fig. 1). Observations are sparse in this region, es-  
 625 pecially for analysis on interannual time scales. We have used a  $1/4^\circ$ -resolution global  
 626 ocean-sea ice model (NorESM) with realistic atmospheric forcing for the period 1973-  
 627 2004. This model represents a typical ocean component of coupled global climate mod-  
 628 els, although with higher resolution. This allows us to analyse drivers of salinity changes  
 629 both on seasonal and interannual time scales. However, the model has biases, such as  
 630 a too saline Greenland shelf between Fram Strait and Denmark Strait, and too fresh Nordic

631 Seas interior (Fig. 5). This results in an underestimation of the liquid freshwater trans-  
 632 ports in Fram Strait and Denmark Strait (Table 1). The solid freshwater transport is  
 633 underestimated to some extent in Fram Strait, but slightly overestimated in Denmark  
 634 Strait. On the other hand, NorESM shows reasonable results for the seasonal shifts in  
 635 the surface salinity in the Greenland and Iceland Seas, and the seasonal cycles of both  
 636 the liquid and solid components in Fram Strait and Denmark Strait are fairly well rep-  
 637 resented.

638 Previous studies suggest that some of the liquid and solid freshwater transported  
 639 by the EGC is diverted into the interior of the Nordic Seas (Dickson et al., 2007; Dodd  
 640 et al., 2009; de Steur et al., 2015; Latarius et al., 2019). In NorESM, we find that solid  
 641 freshwater (sea ice volume flux) is the major source of freshwater to the interior (Fig.  
 642 6), consistent with the results of Dodd et al. (2009). This result is also consistent with  
 643 a recent study by Selyuzhenok et al. (2020), showing that the sea ice volume flux into  
 644 the Greenland Sea is dominating the freshwater budget of the Greenland Sea. The an-  
 645 nual mean solid freshwater diversion in NorESM (19 mSv) amounts to 41% of the an-  
 646 nual mean solid freshwater transport entering through Fram Strait (46.2 mSv). A recent  
 647 study using a very high-resolution model in the Nordic Seas (Spall et al., 2021) comple-  
 648 ments our NorESM results, finding that the annual mean exchange of salt between the  
 649 shelf and the interior in the Greenland Sea is small (considering both mean advection  
 650 and eddy advection).

651 In line with observations, a seasonal migration of the Polar Front is simulated in  
 652 NorESM (Fig. 2). However, the position of the front is not fully aligned with that of the  
 653 observations, which can probably be attributed to the limited horizontal resolution of  
 654 the model. Although our model is relatively coarse, we use the model to test the hypoth-  
 655 esis of Våge et al. (2018); that winds regulate the seasonal migration of the Polar Front.  
 656 Våge et al. (2018) suggested that a westward displacement of the front in the Iceland  
 657 Sea is caused by increased onshore Ekman transport due to enhanced northerly winds  
 658 in fall and winter. In our study, we find that the shifts in the Polar Front not only oc-  
 659 curs in the Iceland Sea, but all along east Greenland north of Denmark Strait. This is  
 660 demonstrated both in observations and in NorESM (Fig. 2). NorESM shows a statis-  
 661 tically significant relationship (correlation  $> 0.5$  at one month lag) between westward  
 662 Ekman transport distance and SSS in the western Nordic Seas (Fig. 10b), and thus sup-  
 663 ports the hypothesis of Våge et al (2018); that the location of the Polar Front is linked  
 664 to the wind forcing.

665 On an interannual time scale, NorESM shows that changes in surface salinity in  
 666 the western Nordic Seas is strongly related to changes in the annual mean solid fresh-  
 667 water diversion (correlation  $< -0.7$ , Fig. 12). Such surface salinity changes take place  
 668 all along east Greenland; an increase in the solid freshwater diversion from the EGC co-  
 669 incides with a negative salinity anomaly in the western Nordic Seas, and visa versa (Fig.  
 670 14a and 14b). The solid freshwater diversion is largest in winter (Dec-Apr, Fig. 8c) and  
 671 the largest salinity anomalies occur in late summer (Jul-Aug-Sep, Fig. 3). This suggests  
 672 that sea ice reaching the interior Nordic Seas melts there during summer and modifies  
 673 the surface salinity in late summer.

674 We find that the main source of sea ice into the interior comes from Fram Strait  
 675 ice export, although another source could also be locally formed sea ice. The observa-  
 676 tion-based study of Venegas and Mysak (2000) found that sea ice variability in the Green-  
 677 land Sea during 1950-1998 was to a large extent explained by variability in ice export  
 678 through Fram Strait and by local wind anomalies during winter. Consistent with that,  
 679 in our model simulation we find that the solid freshwater transport through Fram Strait  
 680 covary to some extent with the diversion into the interior on interannual time scales (cor-  
 681 relation of 0.43 at zero time lag).

682 On even longer time scales, the drivers of salinity changes in this region are sug-  
 683 gested to be rooted in the subpolar North Atlantic and decadal changes in the Atlantic  
 684 inflow into the Nordic Seas (e.g., Glessmer et al., 2014; Lauvset et al., 2018; Kenigson  
 685 & Timmermans, 2021). Thus, main drivers of salinity changes in the western Nordic Seas  
 686 appear to depend on the time scales considered; local winds driving seasonal changes,  
 687 more Arctic-driven interannual changes via sea ice diversion from the EGC, and more  
 688 Atlantic-driven decadal changes via the Atlantic inflow. The time scales of these differ-  
 689 ent mechanisms give an indication of how far ahead we can predict changes in surface  
 690 salinity.

691 Several recent papers demonstrate predictability several years ahead in the upper  
 692 ocean temperature and salinity in the *eastern* Nordic Seas – or more specifically the At-  
 693 lantic domain. This predictability is linked to changes in the properties of Atlantic Wa-  
 694 ter farther upstream (Chafik et al., 2015; Årthun et al., 2017; Langehaug et al., 2019),  
 695 although predictability is limited to some extent by local surface forcing (Asbjørnsen et  
 696 al., 2019). Changes in the properties of the Atlantic Water also influence the *western* Nordic  
 697 Seas – in the Arctic and Polar domains (e.g., Eldevik et al., 2009; Årthun & Eldevik, 2016;  
 698 Lauvset et al., 2018), but the signal is diminished for several reasons, such as mixing with  
 699 the southward-flowing fresh Polar Water (Håvik et al., 2017). Furthermore, the predictabil-  
 700 ity related to the amount of sea ice and liquid freshwater from the Arctic Ocean is lim-  
 701 ited, with predictability only one year ahead (Schmith et al., 2018). This is consistent  
 702 with two studies using dynamical prediction models (Germe et al., 2014; Dai et al., 2020),  
 703 showing some skill in predicting sea ice extent in the Nordic Seas up to only one year  
 704 ahead. Thus, the predictability beyond one year of the upper ocean and sea ice in the  
 705 Polar and Arctic domains appears to be low compared to the predictability in the At-  
 706 lantic domain.

## 707 Appendix A Calculation of liquid freshwater transport

708 In addition to the freshwater transports, we have also looked at the salinity trans-  
 709 ports for the same area. The salinity transport gives reasonable values (about 250kt/s)  
 710 in the western Fram Strait (Schauer & Losch, 2019) and a budget close to balance. The  
 711 incoming salt transport in Fram Strait is balanced by the outgoing salt transport in the  
 712 outer EGC and Denmark Strait. The salt transport in the Iceland section is very small  
 713 due to a very small volume transport.

714 The liquid freshwater transport ( $FWT_{ocean}$ ) is calculated in each of the sections  
 715 shown in Fig. 1. This transport has been calculated in a similar way as in previous ob-  
 716 servational studies of the  $FWT_{ocean}$  through a section north of Denmark Strait (de Steur  
 717 et al., 2017) and through the western Fram Strait (de Steur et al., 2009, 2018). In Equa-  
 718 tion (1), based on the observational studies,  $V$  is volume transport in  $Sv$ ,  $S$  is salinity,  
 719 and the reference salinity ( $S_{ref}$ ) is defined herein as 34.9.

720 However, in this study, we use Equation (2) for the model output. The model out-  
 721 put from NorESM is given as mass flux,  $Mf$  (kg/s), and salt flux,  $Sf$  (kg/s). We ap-  
 722 ply Equation (2) because the nonlinear terms in the salt flux of the ocean model is not  
 723 captured by the formulation  $V \times S$  in Equation (1). For an instantaneous moment in  
 724 time, the two equations are the same (i.e.,  $Sf$  is equal to  $V \times S$ ). However, the model  
 725 output is monthly means and monthly  $Sf$  does not equal  $V \times S$ . In Equation (2) we  
 726 multiply  $Sf$  by  $1000 \text{ kg/m}^3$ , as the modelled  $Sf$  has not been multiplied by the density  
 727 of water during the model run.

$$728 \quad FWT_{ocean} = \int_{x_1}^{x_2} \int_{z(S=S_{ref})}^{z=0} V(x, z) \times \frac{S_{ref} - S(x, z)}{S_{ref}} dz dx \quad (1)$$

$$FWT_{ocean} = \sum_{x1}^{x2} \sum_{z(S=Sref)}^{z=0} Mf(x, z) - \frac{1000 \times Sf(x, z)}{Sref} \quad (2)$$

In order to compare with observational values, we further divide  $FWT_{ocean}$  from the model by a density of  $1000\text{kg/m}^3$  to convert to the unit mSv.

In the literature there are studies that calculate the  $FWT_{ocean}$  as in Equation (2), but without dividing  $Sf$  by  $Sref$ . In this study we want to calculate the  $FWT_{ocean}$  in a similar way to the observational studies in Fram Strait and Denmark Strait, and therefore we divide by  $Sref$ .

We have compared the resulting  $FWT_{ocean}$  of using Equation (1) and Equation (2), and we find that the mean seasonal cycle for the time period 1973-2004 are fairly similar in Denmark Strait (not shown). However, the results are not that similar in Fram Strait, probably because of the more complex ocean circulation in that region. Comparing the resulting interannual variability from the two Equations, we find in general larger variance using Equation (2) and also the timing of the peaks appears to be more realistic compared to the observed  $FWT_{ocean}$  in Fram Strait (de Steur et al., 2009).

## Appendix B Calculation of solid freshwater transport (sea ice volume transport)

The sea ice volume transport,  $VOL_{ice}$ , is calculated in each of the sections shown in Fig. 1, and the general formula is as in Equation (3).

$$VOL_{ice} = hi \times vel \times dx, \quad (3)$$

where  $hi$  is the grid cell mean ice thickness (m),  $vel$  is the ice velocity (m/s), and  $dx$  is size of the grid cell (m).

The sea ice volume transport is converted to a solid freshwater transport,  $FWT_{ice}$ , according to Equation (4). This formula is given in (Curry et al., 2014).

$$FWT_{ice} = VOL_{ice} \times \frac{Sref - S_{ice}}{Sref} \times \frac{\rho_{ice}}{\rho_{water}}, \quad (4)$$

where  $S_{ice} = 5$  (sea ice salinity),  $\rho_{ice} = 900\text{kg/m}^3$  (density of sea ice), and  $\rho_{water} = 1000\text{kg/m}^3$  (density of freshwater).

## Acknowledgments

The research leading to these results has received funding from the Research Council of Norway (RCN) through the project VENTILATE (229791) (HRL, EJ). This is a contribution to the strategic project FRESHWATER (HRL, KV, EJ) of the Bjerknes Centre for Climate Research. HRL has also been funded by the Blue-Action Project (European Union's Horizon 2020 research and innovation program, Grant 727852). KV and AB were funded by the Trond Mohn Foundation under Grant BFS2016REK01. This study has also been supported by the institutional basic funding to the Nansen Center granted by the Research Council of Norway (project no. 218857). Regarding the production of the model experiment used herein, we thank EVA (Earth system modelling of climate Variations in the Anthropocene) with RCN project number 229771.

## Data Availability Statement

Model output from the Bjerknes Centre for Climate Research are archived at Sigma2: The Norwegian e-infrastructure for Research and Education. Information about the model

769 and the version used is given in Section 2.1. The salinity observations used in this study  
770 are described in Huang et al. (2020).

## 771 Tables

**Table 1.** Freshwater transports (only liquid; mSv) in observations and NorESM with the annual mean (*MEAN*) and the maximum value of the mean seasonal cycle (*MAX*) given below. All values using a reference salinity of 34.9 are marked by a star (\*). Otherwise, a reference salinity of 34.8 is used. Most of the observational values include the freshwater transport on the shelf (shown in bold). The model data includes both and cover the period 1973-2004. The maximum value of the simulated seasonal cycle is in October (October and November) in Fram Strait (Denmark Strait).

Strait	$MEAN_{obs}$	$MAX_{obs}$	$MEAN_{model}$	$MAX_{model}$
Fram Strait <sup>a</sup>	<b>70*</b>	> <b>80*</b>	<b>10*</b>	<b>20*</b>
Fram Strait <sup>b</sup>	<b>68.6*</b>			
Denmark Strait <sup>c</sup>	<b>94*</b>	> <b>130*</b>	<b>19*</b>	<b>35*</b>
Denmark Strait <sup>d</sup>		<b>81</b>		
Denmark Strait <sup>e</sup>		55		
Denmark Strait <sup>f</sup>		43-60*		

<sup>a</sup> Observational values from the period 2003-2015. The maximum value is the November value from Fig. 3d in de Steur et al. (2018).

<sup>b</sup> Observational values are updated for the period 2003-2019 (Karpouzoglou et al., 2022).

<sup>c</sup> Observational values from the period Sep 2011 to Jul 2012. The maximum value is the September value from Fig. 7a in de Steur et al. (2017). They assume a contribution from the shelf (20 mSv).

<sup>d</sup> Observational values from summer (Jul-Aug) 2012 (Håvik et al., 2017, their section 3).

<sup>e</sup> Observational values from summer (Jul-Aug) 2004 (Sutherland & Pickart, 2008).

<sup>f</sup> Observational values from Oct 1998 and Aug 1999 (Dodd et al., 2009).

## 772 References

- 773 Årthun, M., & Eldevik, T. (2016). On anomalous ocean heat transport toward the  
774 arctic and associated climate predictability. *Journal of Climate*, 29(2), 689-  
775 704. Retrieved from <http://dx.doi.org/10.1175/JCLI-D-15-0448.1> doi:  
776 10.1175/JCLI-D-15-0448.1
- 777 Årthun, M., Eldevik, T., Viste, E., Drange, H., Furevik, T., Johnson, H. L., &  
778 Keenlyside, N. S. (2017). Skillful prediction of northern climate pro-  
779 vided by the ocean. *Nature Communications*, 8(1), 15875. Retrieved from  
780 <https://doi.org/10.1038/ncomms15875> doi: 10.1038/ncomms15875
- 781 Asbjørnsen, H., Årthun, M., Skagseth, Ø., & Eldevik, T. (2019). Mechanisms of  
782 ocean heat anomalies in the norwegian sea. *Journal of Geophysical Research:*  
783 *Oceans*, 124(4), 2908-2923. Retrieved from [https://agupubs.onlinelibrary](https://agupubs.onlinelibrary.wiley.com/doi/abs/10.1029/2018JC014649)  
784 [.wiley.com/doi/abs/10.1029/2018JC014649](https://agupubs.onlinelibrary.wiley.com/doi/abs/10.1029/2018JC014649) doi: 10.1029/2018JC014649
- 785 Behrendt, A., Sumata, H., Rabe, B., & Schauer, U. (2018). Udash - unified database  
786 for arctic and subarctic hydrography. *Earth System Science Data*, 10(2), 1119-  
787 1138. Retrieved from [https://www.earth-syst-sci-data.net/10/1119/](https://www.earth-syst-sci-data.net/10/1119/2018/)  
788 2018/ doi: 10.5194/essd-10-1119-2018

- 789 Behrens, E., Våge, K., Harden, B., Biastoch, A., & Böning, C. W. (2017).  
 790 Composition and variability of the denmark strait overflow water in a  
 791 high-resolution numerical model hindcast simulation. *Journal of Geo-*  
 792 *physical Research: Oceans*, *122*(4), 2830-2846. Retrieved from [https://](https://agupubs.onlinelibrary.wiley.com/doi/abs/10.1002/2016JC012158)  
 793 [agupubs.onlinelibrary.wiley.com/doi/abs/10.1002/2016JC012158](https://doi.org/10.1002/2016JC012158) doi:  
 794 <https://doi.org/10.1002/2016JC012158>
- 795 Bentsen, M., Bethke, I., Debernard, J. B., Iversen, T., Kirkevåg, A., Seland, Ø.,  
 796 ... Kristjánsson, J. E. (2013). The norwegian earth system model, noresm1-  
 797 m - part 1: Description and basic evaluation of the physical climate. *Geo-*  
 798 *scientific Model Development*, *6*(3), 687-720. Retrieved from [https://](https://www.geosci-model-dev.net/6/687/2013/)  
 799 [www.geosci-model-dev.net/6/687/2013/](https://www.geosci-model-dev.net/6/687/2013/) doi: 10.5194/gmd-6-687-2013
- 800 Brakstad, A., Våge, K., Håvik, L., & Moore, G. W. K. (2019). Water mass transfor-  
 801 mation in the greenland sea during the period 1986–2016. *Journal of Physical*  
 802 *Oceanography*, *49*(1), 121-140. doi: 10.1175/JPO-D-17-0273.1
- 803 Castelao, R. M., Luo, H., Oliver, H., Rennermalm, A. K., Tedesco, M., Bracco,  
 804 A., ... Medeiros, P. M. (2019). Controls on the transport of meltwater  
 805 from the southern greenland ice sheet in the labrador sea. *Journal of Geo-*  
 806 *physical Research: Oceans*, *124*(6), 3551-3560. Retrieved from [https://](https://agupubs.onlinelibrary.wiley.com/doi/abs/10.1029/2019JC015159)  
 807 [agupubs.onlinelibrary.wiley.com/doi/abs/10.1029/2019JC015159](https://doi.org/10.1029/2019JC015159) doi:  
 808 <https://doi.org/10.1029/2019JC015159>
- 809 Chafik, L., Nilsson, J., Skagseth, Ø., & Lundberg, P. (2015). On the flow of atlantic  
 810 water and temperature anomalies in the nordic seas toward the arctic ocean.  
 811 *Journal of Geophysical Research: Oceans*, *120*(12), 7897-7918. Retrieved from  
 812 <http://dx.doi.org/10.1002/2015JC011012> doi: 10.1002/2015JC011012
- 813 Chafik, L., & Rossby, T. (2019). Volume, heat, and freshwater divergences in  
 814 the subpolar north atlantic suggest the nordic seas as key to the state of the  
 815 meridional overturning circulation. *Geophysical Research Letters*, *46*(9), 4799-  
 816 4808. Retrieved from [https://agupubs.onlinelibrary.wiley.com/doi/abs/](https://agupubs.onlinelibrary.wiley.com/doi/abs/10.1029/2019GL082110)  
 817 [10.1029/2019GL082110](https://doi.org/10.1029/2019GL082110) doi: 10.1029/2019GL082110
- 818 Condron, A., Winsor, P., Hill, C., & Menemenlis, D. (2009). Simulated response of  
 819 the arctic freshwater budget to extreme nao wind forcing. *Journal of Climate*,  
 820 *22*(9), 2422 - 2437. Retrieved from [https://journals.ametsoc.org/view/](https://journals.ametsoc.org/view/journals/clim/22/9/2008jcli2626.1.xml)  
 821 [journals/clim/22/9/2008jcli2626.1.xml](https://doi.org/10.1175/2008JCLI2626.1) doi: 10.1175/2008JCLI2626.1
- 822 Curry, B., Lee, C. M., Petrie, B., Moritz, R. E., & Kwok, R. (2014). Multiyear  
 823 volume, liquid freshwater, and sea ice transports through davis strait, 2004–10.  
 824 *Journal of Physical Oceanography*, *44*(4), 1244-1266. Retrieved from [https://](https://doi.org/10.1175/JPO-D-13-0177.1)  
 825 [doi.org/10.1175/JPO-D-13-0177.1](https://doi.org/10.1175/JPO-D-13-0177.1) doi: 10.1175/JPO-D-13-0177.1
- 826 Dai, P., Gao, Y., Counillon, F., Wang, Y., Kimmritz, M., & Langehaug, H. R.  
 827 (2020). Seasonal to decadal predictions of regional arctic sea ice by as-  
 828 simulating sea surface temperature in the norwegian climate prediction  
 829 model. *Climate Dynamics*. Retrieved from [https://doi.org/10.1007/](https://doi.org/10.1007/s00382-020-05196-4)  
 830 [s00382-020-05196-4](https://doi.org/10.1007/s00382-020-05196-4) doi: 10.1007/s00382-020-05196-4
- 831 Danabasoglu, G., Yeager, S. G., Bailey, D., Behrens, E., Bentsen, M., Bi, D., ...  
 832 Wang, Q. (2014, 1). North atlantic simulations in coordinated ocean-  
 833 ice reference experiments phase ii (core-ii). part i: Mean states. *Ocean*  
 834 *Modelling*, *73*, 76-107. Retrieved from [http://www.sciencedirect.com/](http://www.sciencedirect.com/science/article/pii/S1463500313001868)  
 835 [science/article/pii/S1463500313001868](http://dx.doi.org/10.1016/j.ocemod.2013.10.005) doi: [http://dx.doi.org/10.1016/](http://dx.doi.org/10.1016/j.ocemod.2013.10.005)  
 836 [j.ocemod.2013.10.005](http://dx.doi.org/10.1016/j.ocemod.2013.10.005)
- 837 de Steur, L., Hansen, E., Gerdes, R., Karcher, M., Fahrbach, E., & Holfort, J.  
 838 (2009). Freshwater fluxes in the east greenland current: A decade of obser-  
 839 vations. *Geophysical Research Letters*, *36*(23). Retrieved from [https://](https://agupubs.onlinelibrary.wiley.com/doi/abs/10.1029/2009GL041278)  
 840 [agupubs.onlinelibrary.wiley.com/doi/abs/10.1029/2009GL041278](https://doi.org/10.1029/2009GL041278) doi:  
 841 [10.1029/2009GL041278](https://doi.org/10.1029/2009GL041278)
- 842 de Steur, L., Peralta-Ferriz, C., & Pavlova, O. (2018). Freshwater export in the  
 843 east greenland current freshens the north atlantic. *Geophysical Research Let-*

- 844        *ters*, 45(24), 13,359-13,366. doi: 10.1029/2018GL080207
- 845 de Steur, L., Pickart, R. S., Macrander, A., Våge, K., Harden, B., Jónsson, S.,  
846        ... Valdimarsson, H. (2017). Liquid freshwater transport estimates from  
847        the east greenland current based on continuous measurements north of den-  
848        mark strait. *Journal of Geophysical Research: Oceans*, 122(1), 93-109. doi:  
849        10.1002/2016JC012106
- 850 de Steur, L., Pickart, R. S., Torres, D. J., & Valdimarsson, H. (2015). Recent  
851        changes in the freshwater composition east of greenland. *Geophysical Research*  
852        *Letters*, 42(7), 2326-2332. Retrieved from [https://agupubs.onlinelibrary](https://agupubs.onlinelibrary.wiley.com/doi/abs/10.1002/2014GL062759)  
853        [.wiley.com/doi/abs/10.1002/2014GL062759](https://agupubs.onlinelibrary.wiley.com/doi/abs/10.1002/2014GL062759) doi: 10.1002/2014GL062759
- 854 Dickson, R. R., Rudels, B., Dye, S., Karcher, M., Meincke, J., & Yashayaev,  
855        I. (2007). Current estimates of freshwater flux through arctic and sub-  
856        arctic seas. *Progress in Oceanography*, 73(3), 210 - 230. Retrieved from  
857        <http://www.sciencedirect.com/science/article/pii/S007966110700081X>  
858        (Observing and Modelling Ocean Heat and Freshwater Budgets and Trans-  
859        ports) doi: <https://doi.org/10.1016/j.pocean.2006.12.003>
- 860 Dodd, P. A., Heywood, K. J., Meredith, M. P., Naveira-Garabato, A. C., Marca,  
861        A. D., & Falkner, K. K. (2009). Sources and fate of freshwater exported in the  
862        east greenland current. *Geophysical Research Letters*, 36(19). Retrieved  
863        from [https://agupubs.onlinelibrary.wiley.com/doi/abs/10.1029/](https://agupubs.onlinelibrary.wiley.com/doi/abs/10.1029/2009GL039663)  
864        [2009GL039663](https://agupubs.onlinelibrary.wiley.com/doi/abs/10.1029/2009GL039663) doi: 10.1029/2009GL039663
- 865 Eden, C., & Greatbatch, R. J. (2008). Towards a mesoscale eddy closure. *Ocean*  
866        *Modelling*, 20(3), 223 - 239. Retrieved from [http://www.sciencedirect.com/](http://www.sciencedirect.com/science/article/pii/S1463500307001163)  
867        [science/article/pii/S1463500307001163](http://www.sciencedirect.com/science/article/pii/S1463500307001163) doi: [https://doi.org/10.1016/](https://doi.org/10.1016/j.ocemod.2007.09.002)  
868        [j.ocemod.2007.09.002](https://doi.org/10.1016/j.ocemod.2007.09.002)
- 869 Eldevik, T., Nilsen, J. E. Ø., Iovino, D., Anders Olsson, K., Sandø, A. B., & Drange,  
870        H. (2009, 06). Observed sources and variability of nordic seas overflow. *Nature*  
871        *Geosci*, 2(6), 406-410. Retrieved from [http://dx.doi.org/10.1038/](http://dx.doi.org/10.1038/ngeo518)  
872        [ngeo518](http://dx.doi.org/10.1038/ngeo518)
- 873 Fox-Kemper, B., Ferrari, R., & Hallberg, R. (2008). Parameterization of mixed layer  
874        eddies. part i: Theory and diagnosis. *Journal of Physical Oceanography*, 38(6),  
875        1145-1165. Retrieved from <http://dx.doi.org/10.1175/2007JP03792.1> doi:  
876        10.1175/2007JPO3792.1
- 877 Fuentes-Franco, R., & Koenigk, T. (2019). Sensitivity of the arctic freshwater  
878        content and transport to model resolution. *Climate Dynamics*, 53(3), 1765–  
879        1781. Retrieved from <https://doi.org/10.1007/s00382-019-04735-y> doi:  
880        10.1007/s00382-019-04735-y
- 881 Gent, P. R., & McWilliams, J. C. (1990). Isopycnal mixing in ocean circulation  
882        models. *Journal of Physical Oceanography*, 20(1), 150-155. Retrieved from  
883        [http://dx.doi.org/10.1175/1520-0485\(1990\)020<0150:IMIOCM>2.0.CO;2](http://dx.doi.org/10.1175/1520-0485(1990)020<0150:IMIOCM>2.0.CO;2)  
884        doi: 10.1175/1520-0485(1990)020<0150:IMIOCM>2.0.CO;2
- 885 Germe, A., Chevallier, M., Salas y Mélia, D., Sanchez-Gomez, E., & Cassou, C.  
886        (2014). Interannual predictability of arctic sea ice in a global climate model:  
887        regional contrasts and temporal evolution. *Climate Dynamics*, 43(9), 2519–  
888        2538. Retrieved from <https://doi.org/10.1007/s00382-014-2071-2> doi:  
889        10.1007/s00382-014-2071-2
- 890 Glessmer, M. S., Eldevik, T., Våge, K., Øie Nilsen, J. E., & Behrens, E. (2014).  
891        Atlantic origin of observed and modelled freshwater anomalies in the nordic  
892        seas. *Nature Geoscience*, 7(11), 801–805. Retrieved from [https://doi.org/](https://doi.org/10.1038/ngeo2259)  
893        [10.1038/ngeo2259](https://doi.org/10.1038/ngeo2259) doi: 10.1038/ngeo2259
- 894 Gregg, M. C., Sanford, T. B., & Winkel, D. P. (2003). Reduced mixing from the  
895        breaking of internal waves in equatorial waters. *Nature*, 422(6931), 513-515.  
896        Retrieved from <http://dx.doi.org/10.1038/nature01507>
- 897 Guo, C., Ilicak, M., Bentsen, M., & Fer, I. (2016). Characteristics of the nordic  
898        seas overflows in a set of norwegian earth system model experiments. *Ocean*

- 899 *Modelling*, 104, 112-128. Retrieved from <http://www.sciencedirect.com/science/article/pii/S1463500316300543> doi: <http://dx.doi.org/10.1016/j.ocemod.2016.06.004>
- 900
- 901
- 902 Haine, T. W., Curry, B., Gerdes, R., Hansen, E., Karcher, M., Lee, C., ...
- 903 Woodgate, R. (2015). Arctic freshwater export: Status, mechanisms, and
- 904 prospects. *Global and Planetary Change*, 125, 13 - 35. doi: <https://doi.org/10.1016/j.gloplacha.2014.11.013>
- 905
- 906 Hallberg, R. (2013). Using a resolution function to regulate parameterizations of
- 907 oceanic mesoscale eddy effects. *Ocean Modelling*, 72, 92 - 103. Retrieved from
- 908 <http://www.sciencedirect.com/science/article/pii/S1463500313001601>
- 909 doi: <https://doi.org/10.1016/j.ocemod.2013.08.007>
- 910 Hansen, E., Gerland, S., Granskog, M. A., Pavlova, O., Renner, A. H. H., Haapala,
- 911 J., ... Tschudi, M. (2013). Thinning of arctic sea ice observed in fram strait:
- 912 1990–2011. *Journal of Geophysical Research: Oceans*, 118(10), 5202-5221.
- 913 Retrieved from [https://agupubs.onlinelibrary.wiley.com/doi/abs/](https://agupubs.onlinelibrary.wiley.com/doi/abs/10.1002/jgrc.20393)
- 914 [10.1002/jgrc.20393](https://doi.org/10.1002/jgrc.20393) doi: <https://doi.org/10.1002/jgrc.20393>
- 915 Håvik, L., Pickart, R. S., Våge, K., Torres, D., Thurnherr, A. M., Beszczynska-
- 916 Möller, A., ... von Appen, W.-J. (2017). Evolution of the east greenland
- 917 current from fram strait to denmark strait: Synoptic measurements from sum-
- 918 mer 2012. *Journal of Geophysical Research: Oceans*, 122(3), 1974-1994. doi:
- 919 [10.1002/2016JC012228](https://doi.org/10.1002/2016JC012228)
- 920 Huang, J., Pickart, R. S., Huang, R. X., Lin, P., Brakstad, A., & Xu, F. (2020).
- 921 Sources and upstream pathways of the densest overflow water in the nordic
- 922 seas. *Nature Communications*, 11(1), 5389. Retrieved from [https://doi.org/](https://doi.org/10.1038/s41467-020-19050-y)
- 923 [10.1038/s41467-020-19050-y](https://doi.org/10.1038/s41467-020-19050-y) doi: [10.1038/s41467-020-19050-y](https://doi.org/10.1038/s41467-020-19050-y)
- 924 Ikeda, M., Wang, J., & Zhao, J.-P. (2001). Hypersensitive decadal oscillations in
- 925 the arctic/subarctic climate. *Geophysical Research Letters*, 28(7), 1275-1278.
- 926 Retrieved from [https://agupubs.onlinelibrary.wiley.com/doi/abs/](https://agupubs.onlinelibrary.wiley.com/doi/abs/10.1029/2000GL011773)
- 927 [10.1029/2000GL011773](https://doi.org/10.1029/2000GL011773) doi: <https://doi.org/10.1029/2000GL011773>
- 928 Ilıcak, M., Drange, H., Wang, Q., Gerdes, R., Aksenov, Y., Bailey, D., ... Yea-
- 929 ger, S. G. (2016, 4). An assessment of the arctic ocean in a suite of inter-
- 930 annual core-ii simulations. part iii: Hydrography and fluxes. *Ocean Mod-*
- 931 *elling*, 100, 141-161. Retrieved from [http://www.sciencedirect.com/](http://www.sciencedirect.com/science/article/pii/S1463500316000238)
- 932 [science/article/pii/S1463500316000238](http://www.sciencedirect.com/science/article/pii/S1463500316000238) doi: [http://dx.doi.org/10.1016/](http://dx.doi.org/10.1016/j.ocemod.2016.02.004)
- 933 [j.ocemod.2016.02.004](http://dx.doi.org/10.1016/j.ocemod.2016.02.004)
- 934 Ilıcak, M., Özgökmen, T. M., Peters, H., Baumert, H. Z., & Iskandarani, M. (2008).
- 935 Performance of two-equation turbulence closures in three-dimensional sim-
- 936 ulations of the red sea overflow. *Ocean Modelling*, 24(3), 122 - 139. Re-
- 937 trievied from [http://www.sciencedirect.com/science/article/pii/](http://www.sciencedirect.com/science/article/pii/S1463500308000838)
- 938 [S1463500308000838](http://www.sciencedirect.com/science/article/pii/S1463500308000838) doi: <https://doi.org/10.1016/j.ocemod.2008.06.001>
- 939 Ionita, M., Scholz, P., Lohmann, G., Dima, M., & Prange, M. (2016). Linkages be-
- 940 tween atmospheric blocking, sea ice export through fram strait and the atlantic
- 941 meridional overturning circulation. *Scientific Reports*, 6(1), 32881. Retrieved
- 942 from <https://doi.org/10.1038/srep32881> doi: [10.1038/srep32881](https://doi.org/10.1038/srep32881)
- 943 Jeansson, E., Jutterström, S., Rudels, B., Anderson, L. G., Olsson, K. A., Jones,
- 944 E. P., ... Swift, J. H. (2008). Sources to the east greenland current and its
- 945 contribution to the denmark strait overflow. *Progress in Oceanography*, 78(1),
- 946 12 - 28. Retrieved from [http://www.sciencedirect.com/science/article/](http://www.sciencedirect.com/science/article/pii/S0079661108000803)
- 947 [pii/S0079661108000803](http://www.sciencedirect.com/science/article/pii/S0079661108000803) doi: <https://doi.org/10.1016/j.pocean.2007.08.031>
- 948 Karpouzoglou, T., de Steur, L., Smedsrud, L. H., & Sumata, H. (2022). Observed
- 949 changes in the arctic freshwater outflow in fram strait. *Journal of Geophys-*
- 950 *ical Research: Oceans*, 127(3), e2021JC018122. Retrieved from [https://](https://agupubs.onlinelibrary.wiley.com/doi/abs/10.1029/2021JC018122)
- 951 [agupubs.onlinelibrary.wiley.com/doi/abs/10.1029/2021JC018122](https://agupubs.onlinelibrary.wiley.com/doi/abs/10.1029/2021JC018122)
- 952 (e2021JC018122 2021JC018122) doi: <https://doi.org/10.1029/2021JC018122>
- 953 Karstensen, J., Schlosser, P., Wallace, D. W. R., Bullister, J. L., & Blindheim, J.

- 954 (2005). Water mass transformation in the greenland sea during the 1990s.  
 955 *Journal of Geophysical Research: Oceans*, 110(C7). Retrieved from [https://](https://agupubs.onlinelibrary.wiley.com/doi/abs/10.1029/2004JC002510)  
 956 [agupubs.onlinelibrary.wiley.com/doi/abs/10.1029/2004JC002510](https://agupubs.onlinelibrary.wiley.com/doi/abs/10.1029/2004JC002510) doi:  
 957 10.1029/2004JC002510
- 958 Kenigson, J. S., & Timmermans, M.-L. (2021). Nordic seas hydrography in the  
 959 context of arctic and north atlantic ocean dynamics. *Journal of Physi-*  
 960 *cal Oceanography*, 51(1), 101 - 114. Retrieved from [https://journals](https://journals.ametsoc.org/view/journals/phoc/51/1/jpo-d-20-0071.1.xml)  
 961 [.ametsoc.org/view/journals/phoc/51/1/jpo-d-20-0071.1.xml](https://journals.ametsoc.org/view/journals/phoc/51/1/jpo-d-20-0071.1.xml) doi:  
 962 10.1175/JPO-D-20-0071.1
- 963 Khosravi, N., Wang, Q., Koldunov, N., Hinrichs, C., Semmler, T., Danilov, S., &  
 964 Jung, T. (2022). The arctic ocean in cmip6 models: Biases and projected  
 965 changes in temperature and salinity. *Earth's Future*, 10(2), e2021EF002282.  
 966 Retrieved from [https://agupubs.onlinelibrary.wiley.com/doi/abs/](https://agupubs.onlinelibrary.wiley.com/doi/abs/10.1029/2021EF002282)  
 967 [10.1029/2021EF002282](https://agupubs.onlinelibrary.wiley.com/doi/abs/10.1029/2021EF002282) (e2021EF002282 2021EF002282) doi: [https://](https://doi.org/10.1029/2021EF002282)  
 968 [doi.org/10.1029/2021EF002282](https://doi.org/10.1029/2021EF002282)
- 969 Koszalka, I., LaCasce, J., Andersson, M., Orvik, K., & Mauritzen, C. (2011). Sur-  
 970 face circulation in the nordic seas from clustered drifters. *Deep Sea Research*  
 971 *Part I: Oceanographic Research Papers*, 58(4), 468 - 485. Retrieved from  
 972 <http://www.sciencedirect.com/science/article/pii/S0967063711000306>  
 973 doi: <https://doi.org/10.1016/j.dsr.2011.01.007>
- 974 Kwok, R. (2009). Outflow of arctic ocean sea ice into the greenland and barents  
 975 seas: 1979–2007. *Journal of Climate*, 22(9), 2438-2457.
- 976 Lambert, E., Eldevik, T., & Haugan, P. M. (2016). How northern freshwater in-  
 977 put can stabilise thermohaline circulation. *Tellus A: Dynamic Meteorology and*  
 978 *Oceanography*, 68(1), 31051. doi: 10.3402/tellusa.v68.31051
- 979 Lambert, E., Eldevik, T., & Spall, M. A. (2018). On the dynamics and water mass  
 980 transformation of a boundary current connecting alpha and beta oceans. *Jour-*  
 981 *nal of Physical Oceanography*, 48(10), 2457-2475. doi: 10.1175/JPO-D-17-0186  
 982 .1
- 983 Langehaug, H. R., Geyer, F., Smedsrud, L., & Gao, Y. (2013). Arctic sea ice decline  
 984 and ice export in the cmip5 historical simulations. *Ocean Modelling*, 71(0), 114  
 985 - 126. doi: <http://dx.doi.org/10.1016/j.ocemod.2012.12.006>
- 986 Langehaug, H. R., Sandø, A. B., Årthun, M., & Ilcak, M. (2019). Variability  
 987 along the atlantic water pathway in the forced norwegian earth system model.  
 988 *Climate Dynamics*, 52(1), 1211-1230. Retrieved from [https://doi.org/](https://doi.org/10.1007/s00382-018-4184-5)  
 989 [10.1007/s00382-018-4184-5](https://doi.org/10.1007/s00382-018-4184-5) doi: 10.1007/s00382-018-4184-5
- 990 Large, W. G., & Yeager, S. G. (2009). The global climatology of an interannually  
 991 varying air-sea flux data set. *Climate Dynamics*, 33(2), 341-364. Retrieved  
 992 from <http://dx.doi.org/10.1007/s00382-008-0441-3> doi: 10.1007/s00382  
 993 -008-0441-3
- 994 Latarius, K., Schauer, U., & Wisotzki, A. (2019). Near-ice hydrographic  
 995 data from seaglider missions in the western greenland sea in summer 2014  
 996 and 2015. *Earth System Science Data*, 11(2), 895-920. Retrieved from  
 997 <https://www.earth-syst-sci-data.net/11/895/2019/> doi: 10.5194/  
 998 [essd-11-895-2019](https://www.earth-syst-sci-data.net/11/895/2019/)
- 999 Lauvset, S. K., Brakstad, A., Våge, K., Olsen, A., Jeansson, E., & Mork, K. A.  
 1000 (2018). Continued warming, salinification and oxygenation of the greenland  
 1001 sea gyre. *Tellus A: Dynamic Meteorology and Oceanography*, 70(1), 1-9.  
 1002 Retrieved from <https://doi.org/10.1080/16000870.2018.1476434> doi:  
 1003 10.1080/16000870.2018.1476434
- 1004 Legg, S., Hallberg, R. W., & Girton, J. B. (2006). Comparison of entrain-  
 1005 ment in overflows simulated by z-coordinate, isopycnal and non-hydrostatic  
 1006 models. *Ocean Modelling*, 11(1-2), 69-97. Retrieved from [http://](http://www.sciencedirect.com/science/article/pii/S1463500304001064)  
 1007 [www.sciencedirect.com/science/article/pii/S1463500304001064](http://www.sciencedirect.com/science/article/pii/S1463500304001064) doi:  
 1008 <http://dx.doi.org/10.1016/j.ocemod.2004.11.006>

- 1009 Macrander, A., Valdimarsson, H., & Jónsson, S. (2014). Improved transport esti-  
 1010 mate of the east icelandic current 2002–2012. *Journal of Geophysical Research:*  
 1011 *Oceans*, 119(6), 3407-3424. Retrieved from [https://agupubs.onlinelibrary](https://agupubs.onlinelibrary.wiley.com/doi/abs/10.1002/2013JC009517)  
 1012 [.wiley.com/doi/abs/10.1002/2013JC009517](https://agupubs.onlinelibrary.wiley.com/doi/abs/10.1002/2013JC009517) doi: 10.1002/2013JC009517
- 1013 Marsh, R., Desbruyères, D., Bamber, J. L., de Cuevas, B. A., Coward, A. C., &  
 1014 Aksenov, Y. (2010). Short-term impacts of enhanced greenland freshwater  
 1015 fluxes in an eddy-permitting ocean model. *Ocean Science*, 6(3), 749–760.  
 1016 Retrieved from <https://os.copernicus.org/articles/6/749/2010/> doi:  
 1017 10.5194/os-6-749-2010
- 1018 Martínez-Moreno, J., Hogg, A. M., Kiss, A. E., Constantinou, N. C., & Morrison,  
 1019 A. K. (2019). Kinetic energy of eddy-like features from sea surface altime-  
 1020 try. *Journal of Advances in Modeling Earth Systems*, 11(10), 3090-3105.  
 1021 Retrieved from [https://agupubs.onlinelibrary.wiley.com/doi/abs/](https://agupubs.onlinelibrary.wiley.com/doi/abs/10.1029/2019MS001769)  
 1022 [10.1029/2019MS001769](https://agupubs.onlinelibrary.wiley.com/doi/abs/10.1029/2019MS001769) doi: <https://doi.org/10.1029/2019MS001769>
- 1023 Mastropole, D., Pickart, R. S., Valdimarsson, H., Våge, K., Jochumsen, K., &  
 1024 Girtton, J. (2017). On the hydrography of denmark strait. *Journal of*  
 1025 *Geophysical Research: Oceans*, 122(1), 306-321. Retrieved from [https://](https://agupubs.onlinelibrary.wiley.com/doi/abs/10.1002/2016JC012007)  
 1026 [agupubs.onlinelibrary.wiley.com/doi/abs/10.1002/2016JC012007](https://agupubs.onlinelibrary.wiley.com/doi/abs/10.1002/2016JC012007) doi:  
 1027 10.1002/2016JC012007
- 1028 Mauritzen, C. (1996). Production of dense overflow waters feeding the north at-  
 1029 lantic across the greenland-scotland ridge. part 1: Evidence for a revised  
 1030 circulation scheme. *Deep Sea Research Part I: Oceanographic Research Pa-*  
 1031 *pers*, 43(6), 769 - 806. Retrieved from [http://www.sciencedirect.com/](http://www.sciencedirect.com/science/article/pii/0967063796000374)  
 1032 [science/article/pii/0967063796000374](http://www.sciencedirect.com/science/article/pii/0967063796000374) doi: [http://dx.doi.org/10.1016/](http://dx.doi.org/10.1016/0967-0637(96)00037-4)  
 1033 [0967-0637\(96\)00037-4](http://dx.doi.org/10.1016/0967-0637(96)00037-4)
- 1034 Nøst, O. A., & Isachsen, P. E. (2003). The large-scale time-mean ocean cir-  
 1035 culation in the nordic seas and arctic ocean estimated from simplified dy-  
 1036 namics. *Journal of Marine Research*, 61(2), 175-210. Retrieved from  
 1037 [https://www.ingentaconnect.com/content/jmr/jmr/2003/00000061/](https://www.ingentaconnect.com/content/jmr/jmr/2003/00000061/00000002/art00002)  
 1038 [00000002/art00002](https://www.ingentaconnect.com/content/jmr/jmr/2003/00000061/00000002/art00002) doi: doi:10.1357/002224003322005069
- 1039 Nurser, A. J. G., & Bacon, S. (2014). The rossby radius in the arctic ocean. *Ocean*  
 1040 *Science*, 10(6), 967–975. Retrieved from [https://os.copernicus.org/](https://os.copernicus.org/articles/10/967/2014/)  
 1041 [articles/10/967/2014/](https://os.copernicus.org/articles/10/967/2014/) doi: 10.5194/os-10-967-2014
- 1042 Oberhuber, J. M. (1993). Simulation of the atlantic circulation with a coupled  
 1043 sea ice-mixed layer-isopycnal general circulation model. part i: Model descrip-  
 1044 tion. *Journal of Physical Oceanography*, 23(5), 808-829. Retrieved from  
 1045 [http://dx.doi.org/10.1175/1520-0485\(1993\)023<0808:SOTACW>2.0.CO;2](http://dx.doi.org/10.1175/1520-0485(1993)023<0808:SOTACW>2.0.CO;2)  
 1046 doi: 10.1175/1520-0485(1993)023<0808:SOTACW>2.0.CO;2
- 1047 Olsson, K. A., Jeansson, E., Tanhua, T., & Gascard, J.-C. (2005). The east  
 1048 greenland current studied with cfc3 and released sulphur hexafluoride.  
 1049 *Journal of Marine Systems*, 55(1), 77 - 95. Retrieved from [http://](http://www.sciencedirect.com/science/article/pii/S0924796304002568)  
 1050 [www.sciencedirect.com/science/article/pii/S0924796304002568](http://www.sciencedirect.com/science/article/pii/S0924796304002568) doi:  
 1051 <https://doi.org/10.1016/j.jmarsys.2004.07.019>
- 1052 Rudels, B., Björk, G., Nilsson, J., Winsor, P., Lake, I., & Nohr, C. (2005). The  
 1053 interaction between waters from the arctic ocean and the nordic seas north of  
 1054 fram strait and along the east greenland current: results from the arctic ocean-  
 1055 02 oden expedition. *Journal of Marine Systems*, 55(1), 1 - 30. Retrieved from  
 1056 <http://www.sciencedirect.com/science/article/pii/S0924796304002015>  
 1057 doi: <https://doi.org/10.1016/j.jmarsys.2004.06.008>
- 1058 Schauer, U., & Losch, M. (2019). “freshwater” in the ocean is not a useful parameter  
 1059 in climate research. *Journal of Physical Oceanography*, 49(9), 2309-2321. Re-  
 1060 trieved from <https://doi.org/10.1175/JPO-D-19-0102.1> doi: 10.1175/JPO  
 1061 -D-19-0102.1
- 1062 Schmith, T., Olsen, S. M., Ringgaard, I. M., & May, W. (2018). Limited predictabil-  
 1063 ity of extreme decadal changes in the arctic ocean freshwater content. *Climate*

- 1064 *Dynamics*, 51(9), 3927-3942. Retrieved from <https://doi.org/10.1007/s00382-018-4120-8> doi: 10.1007/s00382-018-4120-8
- 1065
- 1066 Schulze Chretien, L. M., & Frajka-Williams, E. (2018). Wind-driven transport  
1067 of fresh shelf water into the upper 30 m of the labrador sea. *Ocean Science*,  
1068 14(5), 1247–1264. Retrieved from [https://os.copernicus.org/articles/](https://os.copernicus.org/articles/14/1247/2018/)  
1069 14/1247/2018/ doi: 10.5194/os-14-1247-2018
- 1070 Selyuzhenok, V., Bashmachnikov, I., Ricker, R., Vesman, A., & Bobylev, L.  
1071 (2020). Sea ice volume variability and water temperature in the green-  
1072 land sea. *The Cryosphere*, 14(2), 477-495. Retrieved from [https://](https://www.the-cryosphere.net/14/477/2020/)  
1073 [www.the-cryosphere.net/14/477/2020/](https://www.the-cryosphere.net/14/477/2020/) doi: 10.5194/tc-14-477-2020
- 1074 Sgubin, G., Swingedouw, D., Drijfhout, S., Mary, Y., & Bennabi, A. (2017). Abrupt  
1075 cooling over the north atlantic in modern climate models. *Nature Communica-*  
1076 *tions*, 8(1), 14375. doi: 10.1038/ncomms14375
- 1077 Simmons, H. L., Jayne, S. R., Laurent, L. C. S., & Weaver, A. J. (2004). Tidally  
1078 driven mixing in a numerical model of the ocean general circulation. *Ocean*  
1079 *Modelling*, 6(3-4), 245-263. Retrieved from [http://www.sciencedirect.com/](http://www.sciencedirect.com/science/article/pii/S1463500303000118)  
1080 [science/article/pii/S1463500303000118](http://www.sciencedirect.com/science/article/pii/S1463500303000118) doi: [http://dx.doi.org/10.1016/](http://dx.doi.org/10.1016/S1463-5003(03)00011-8)  
1081 [S1463-5003\(03\)00011-8](http://dx.doi.org/10.1016/S1463-5003(03)00011-8)
- 1082 Smedsrud, L. H., Sorteberg, A., & Kloster, K. (2008). Recent and future changes of  
1083 the arctic sea-ice cover. *Geophys. Res. Lett.*, 35.
- 1084 Spall, M. A., Almansi, M., Huang, J., Haine, T. W., & Pickart, R. S. (2021). Lat-  
1085 eral redistribution of heat and salt in the nordic seas. *Progress in Oceanog-*  
1086 *raphy*, 196, 102609. Retrieved from [https://www.sciencedirect.com/](https://www.sciencedirect.com/science/article/pii/S0079661121000963)  
1087 [science/article/pii/S0079661121000963](https://www.sciencedirect.com/science/article/pii/S0079661121000963) doi: [https://doi.org/10.1016/](https://doi.org/10.1016/j.pocean.2021.102609)  
1088 [j.pocean.2021.102609](https://doi.org/10.1016/j.pocean.2021.102609)
- 1089 Sutherland, D. A., & Pickart, R. S. (2008). The east greenland coastal current:  
1090 Structure, variability, and forcing. *Progress in Oceanography*, 78(1), 58 - 77.  
1091 Retrieved from [http://www.sciencedirect.com/science/article/pii/](http://www.sciencedirect.com/science/article/pii/S0079661108000864)  
1092 [S0079661108000864](http://www.sciencedirect.com/science/article/pii/S0079661108000864) doi: <https://doi.org/10.1016/j.pocean.2007.09.006>
- 1093 Swift, J. H., & Aagaard, K. (1981). Seasonal transitions and water mass for-  
1094 mation in the iceland and greenland seas. *Deep Sea Research Part A.*  
1095 *Oceanographic Research Papers*, 28(10), 1107 - 1129. Retrieved from  
1096 <http://www.sciencedirect.com/science/article/pii/0198014981900509>  
1097 doi: [https://doi.org/10.1016/0198-0149\(81\)90050-9](https://doi.org/10.1016/0198-0149(81)90050-9)
- 1098 Trodahl, M., & Isachsen, P. E. (2018). Topographic influence on baroclinic insta-  
1099 bility and the mesoscale eddy field in the northern north atlantic ocean and  
1100 the nordic seas. *Journal of Physical Oceanography*, 48(11), 2593 - 2607. Re-  
1101 trieved from [https://journals.ametsoc.org/view/journals/phoc/48/11/](https://journals.ametsoc.org/view/journals/phoc/48/11/jpo-d-17-0220.1.xml)  
1102 [jpo-d-17-0220.1.xml](https://journals.ametsoc.org/view/journals/phoc/48/11/jpo-d-17-0220.1.xml) doi: 10.1175/JPO-D-17-0220.1
- 1103 Våge, K., Moore, G., Jónsson, S., & Valdimarsson, H. (2015). Water mass transfor-  
1104 mation in the iceland sea. *Deep Sea Research Part I: Oceanographic Research*  
1105 *Papers*, 101, 98 - 109. Retrieved from [http://www.sciencedirect.com/](http://www.sciencedirect.com/science/article/pii/S0967063715000680)  
1106 [science/article/pii/S0967063715000680](http://www.sciencedirect.com/science/article/pii/S0967063715000680) doi: [https://doi.org/10.1016/](https://doi.org/10.1016/j.dsr.2015.04.001)  
1107 [j.dsr.2015.04.001](https://doi.org/10.1016/j.dsr.2015.04.001)
- 1108 Våge, K., Papritz, L., Håvik, L., Spall, M. A., & Moore, G. W. K. (2018). Ocean  
1109 convection linked to the recent ice edge retreat along east greenland. *Nature*  
1110 *Communications*, 9(1), 1287. Retrieved from [https://doi.org/10.1038/](https://doi.org/10.1038/s41467-018-03468-6)  
1111 [s41467-018-03468-6](https://doi.org/10.1038/s41467-018-03468-6) doi: 10.1038/s41467-018-03468-6
- 1112 Venegas, S. A., & Mysak, L. A. (2000). Is there a dominant timescale of natu-  
1113 ral climate variability in the arctic? *Journal of Climate*, 13(19), 3412-3434.  
1114 Retrieved from [https://doi.org/10.1175/1520-0442\(2000\)013<3412:](https://doi.org/10.1175/1520-0442(2000)013<3412:ITADTO>2.0.CO;2)  
1115 [ITADTO>2.0.CO;2](https://doi.org/10.1175/1520-0442(2000)013<3412:ITADTO>2.0.CO;2) doi: 10.1175/1520-0442(2000)013(3412:ITADTO)2.0.CO;2
- 1116 Vinje, T. (2001). Fram strait ice fluxes and atmospheric circulation: 1950–2000.  
1117 *Journal of Climate*, 14(16), 3508-3517. doi: 10.1175/1520-0442(2001)014(3508:  
1118 FSIFAA)2.0.CO;2

- 1119 Voet, G., Quadfasel, D., Mork, K. A., & S oiland, H. (2010). The mid-depth circu-  
 1120 lation of the nordic seas derived from profiling float observations. *Tellus A*,  
 1121 *62*(4), 516-529. Retrieved from [https://onlinelibrary.wiley.com/doi/](https://onlinelibrary.wiley.com/doi/abs/10.1111/j.1600-0870.2010.00444.x)  
 1122 [abs/10.1111/j.1600-0870.2010.00444.x](https://onlinelibrary.wiley.com/doi/abs/10.1111/j.1600-0870.2010.00444.x) doi: 10.1111/j.1600-0870.2010  
 1123 .00444.x
- 1124 Weijer, W., Cheng, W., Garuba, O. A., Hu, A., & Nadiga, B. T. (2020). Cmp6  
 1125 models predict significant 21st century decline of the atlantic meridional over-  
 1126 turning circulation. *Geophysical Research Letters*, *47*(12), e2019GL086075.  
 1127 Retrieved from [https://agupubs.onlinelibrary.wiley.com/doi/abs/](https://agupubs.onlinelibrary.wiley.com/doi/abs/10.1029/2019GL086075)  
 1128 [10.1029/2019GL086075](https://agupubs.onlinelibrary.wiley.com/doi/abs/10.1029/2019GL086075) (e2019GL086075 10.1029/2019GL086075) doi:  
 1129 <https://doi.org/10.1029/2019GL086075>
- 1130 Zamani, B., Krumpen, T., Smedsrud, L. H., & Gerdes, R. (2019). Fram strait sea  
 1131 ice export affected by thinning: comparing high-resolution simulations and  
 1132 observations. *Climate Dynamics*, *53*(5), 3257-3270. Retrieved from [https://](https://doi.org/10.1007/s00382-019-04699-z)  
 1133 [doi.org/10.1007/s00382-019-04699-z](https://doi.org/10.1007/s00382-019-04699-z) doi: 10.1007/s00382-019-04699-z

#### 1134 Additional references

- 1135 IPCC, 2019: IPCC Special Report on the Ocean and Cryosphere in a Changing Cli-  
 1136 mate [H.-O. P ortner, D.C. Roberts, V. Masson-Delmotte, P. Zhai, M. Tignor, E. Poloczan-  
 1137 ska, K. Mintenbeck, A. Alegr a, M. Nicolai, A. Okem, J. Petzold, B. Rama, N.M. Weyer  
 1138 (eds.)].
- 1139 Helland-Hansen, B., and F. Nansen, 1909: The Norwegian Sea, its physical oceanog-  
 1140 raphy based upon the Norwegian Researches 1900-1904. Report on Norwegian and Ma-  
 1141 rine Investigations, 2, 390 pp.
- 1142 Large WG, Yeager S (2004) Diurnal to decadal global forcing for ocean and sea-  
 1143 ice models: The data sets and flux climatologies. NCAR Technical Note NCAR/TN-460+STR.  
 1144 <https://doi.org/10.5065/D6KK98Q6>
- 1145 Smagorinsky, J., Large eddy simulation of complex engineering and geophysical flows,  
 1146 in *Evolution of Physical Oceanography*, edited by B. Galperin, and S. A. Orszag, pp. 3-  
 1147 36. Cambridge University Press, 1993.

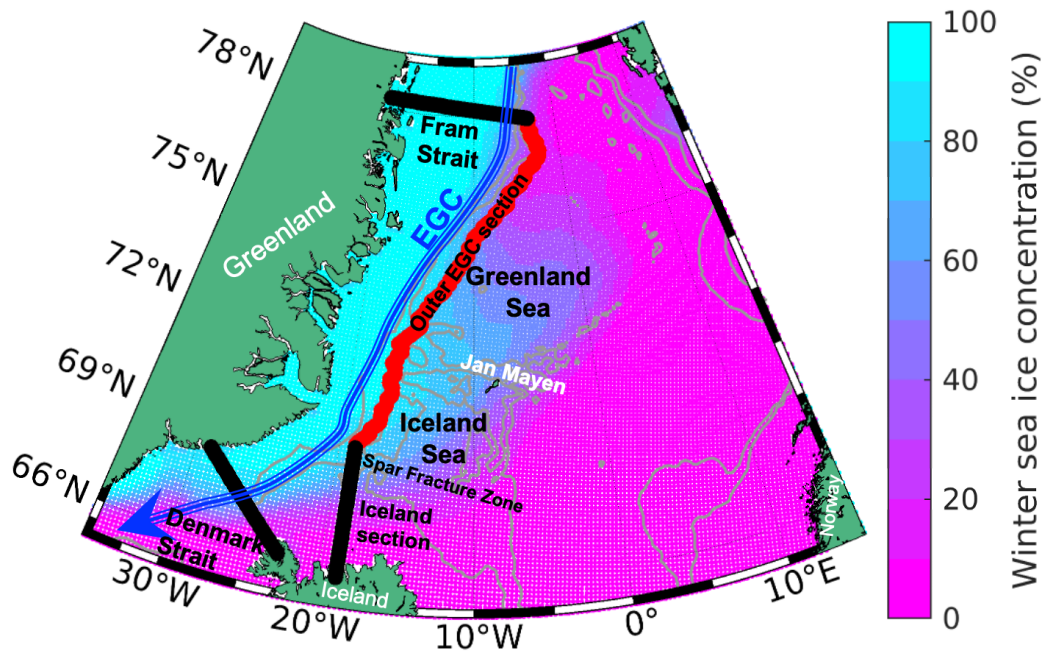


**Figure 1.** The focus region of this study is the western Nordic Seas; encompassing the East Greenland Current (EGC), carrying freshwater and sea ice southward, and the Greenland and Iceland Seas. The three sections marked in black are referred to in the text as the Fram Strait, the Denmark Strait and the Iceland section. The section in red is aligned with the EGC but outside of the main core, i.e., outside the location of maximum velocities. The colour shading is the mean simulated winter (Jan-Feb-Mar) sea ice concentration for the period 1973-2004 from the forced global ocean-ice model used in this study. The depth contours are 1200 and 2000m (thin grey lines).

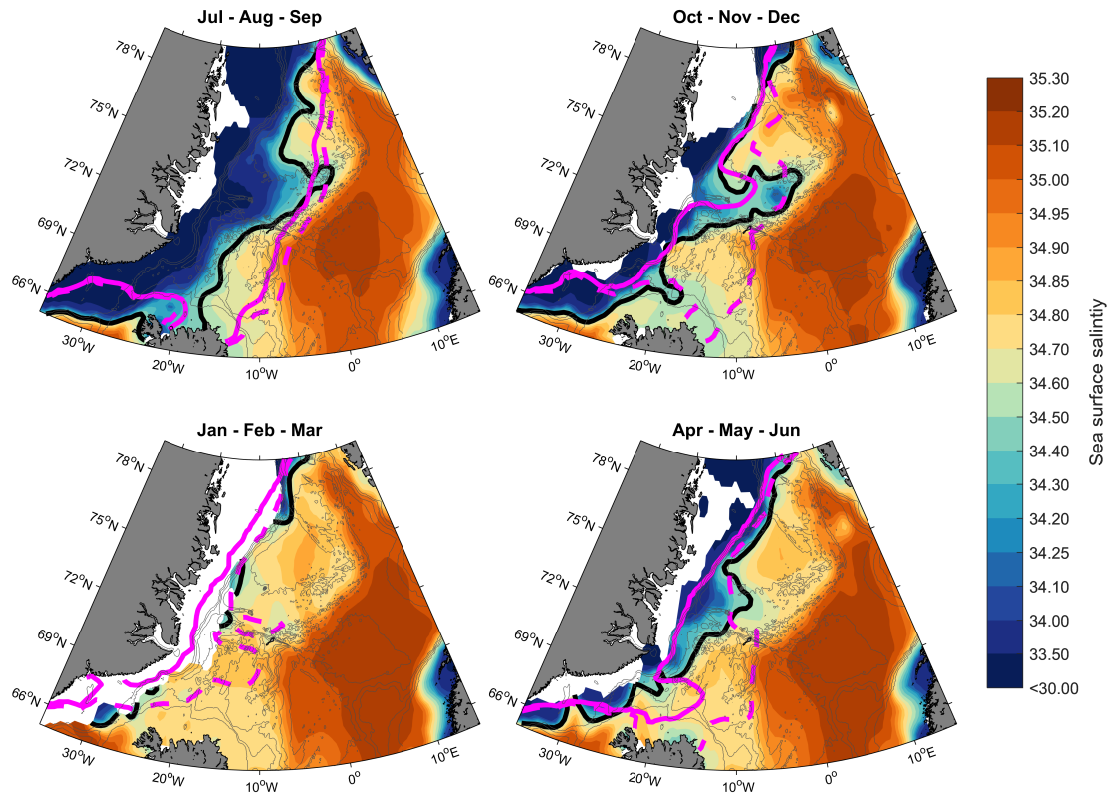


**Figure 2.** Seasonal variability in surface salinity (averaged over the upper 50m) based on observations (Huang et al., 2020) for the period 1986-2016. The solid black line shows the  $S=34.5$  isohaline, which marks the Polar Front. The solid (dashed) magenta lines show the simulated  $S=34.3$  ( $S=34.5$ ) isohaline for the period 1986-2004. The depth contours are 500, 1000, 1500, 2000, 3000, and 4000m (thin grey lines).

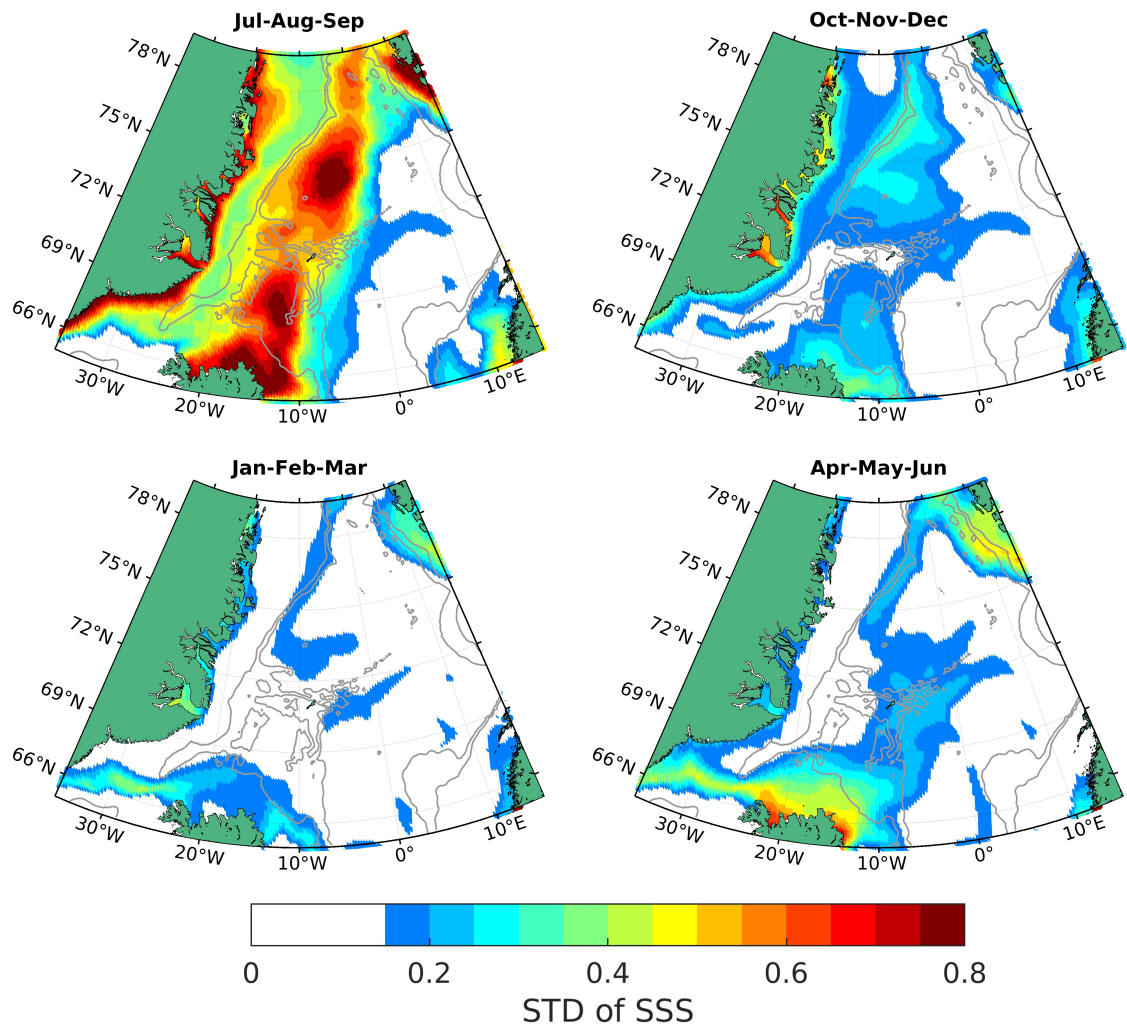


**Figure 3.** Standard deviation of simulated Sea Surface Salinity (SSS) in NorESM for the period 1973-2004 for four different seasons (all time series are detrended). The depth contours are 1200 and 2000m (thin grey lines).

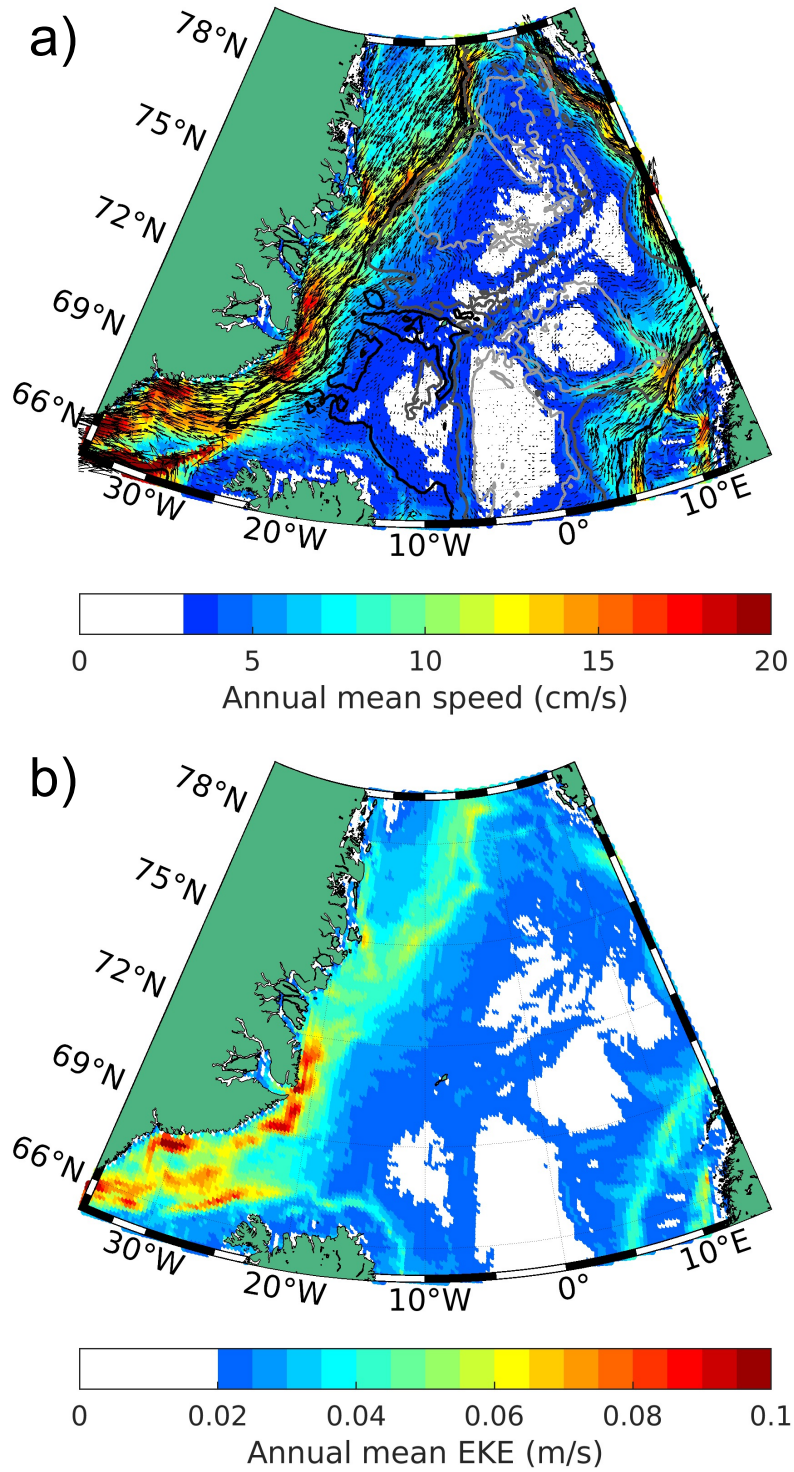


**Figure 4.** a) Simulated mixed-layer velocity in NorESM, showing the annual average over the period 1973-2004. The direction of the currents is shown by the black arrows and the mean speed is shown by colour. The simulated East Greenland Current is shown as a strong southward current in the westernmost part of the Nordic Seas. The depth contours are 1200 (black line), 2000, and 3000m (grey lines). b) Simulated Eddy Kinetic Energy (EKE) using mixed layer velocities.

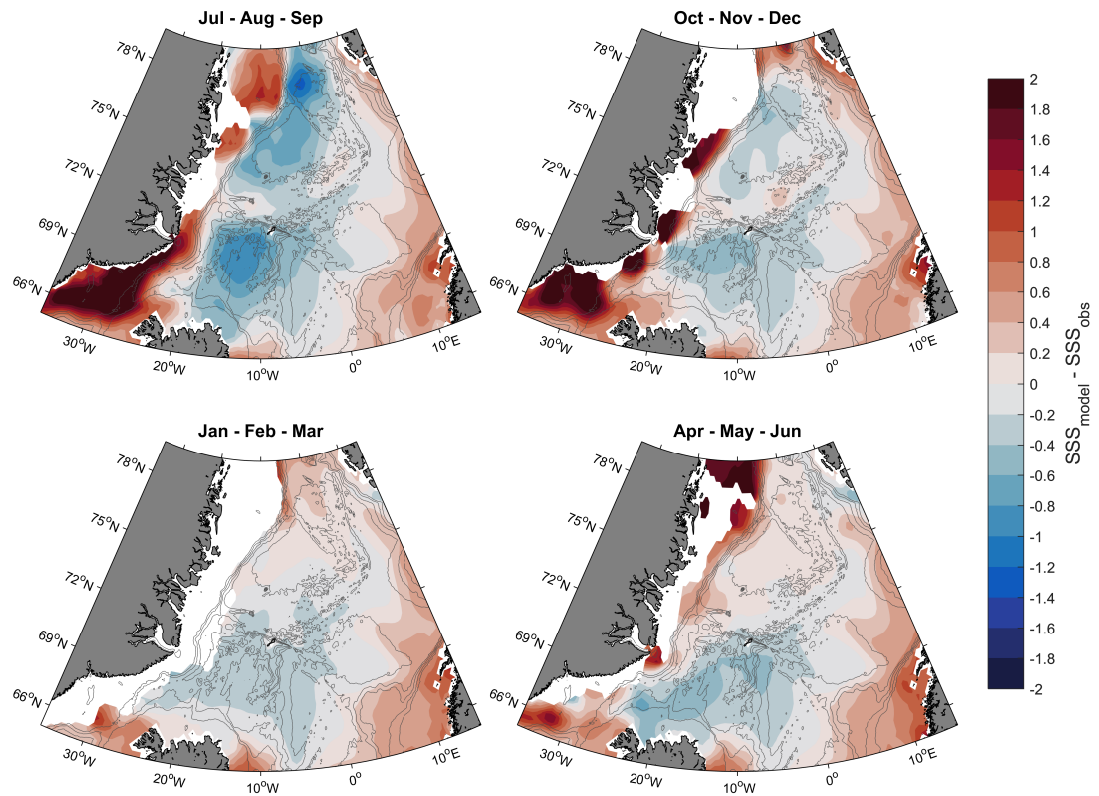


**Figure 5.** The seasonal differences between observed and simulated surface salinity (model minus observations). The depth contours are 500, 1000, 1500, 2000, 3000, and 4000m (thin grey lines).

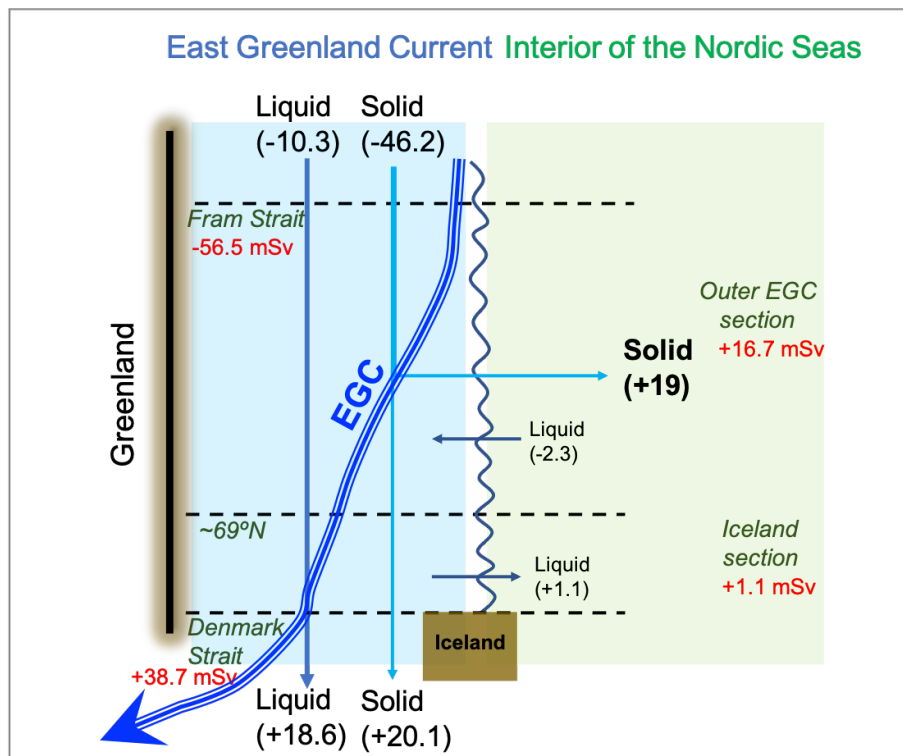


**Figure 6.** Schematic of the freshwater budget in the model simulation for the region enclosed by the four sections: Fram Strait, Denmark Strait, outer EGC section, and Iceland section (the two latter are separated at about 69°N). The annual mean liquid and solid freshwater transports for the period 1973-2004 are shown in black (numbers in mSv), and the total freshwater transport (liquid + solid) across each section is given by the red numbers. The schematic is adopted after Dodd et al. (2009).

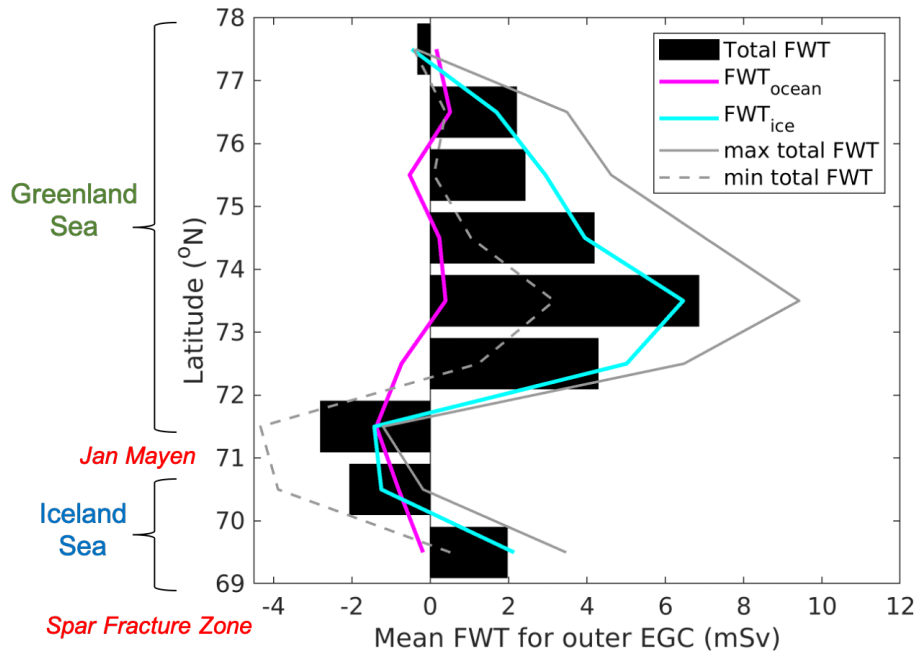


**Figure 7.** The total simulated freshwater transport (FWT) across the outer EGC section, as a function of latitude, given as the annual mean for the period 1973-2004. Positive values mean that there is a total FWT towards the east (the interior of the Nordic Seas). Negative values mean that there is a total FWT towards the west (the Greenland shelf). The liquid freshwater transport (FWT<sub>ocean</sub>) and solid freshwater transport (FWT<sub>ice</sub>) are also shown. In addition, the latitudinal distribution of the total FWT for two different cases are shown (see the red and blue points in Fig. 13). The approximate locations for the Greenland and Iceland Seas are indicated, separated by Jan Mayen. The outer EGC section ends just north of the Spar Fracture Zone.

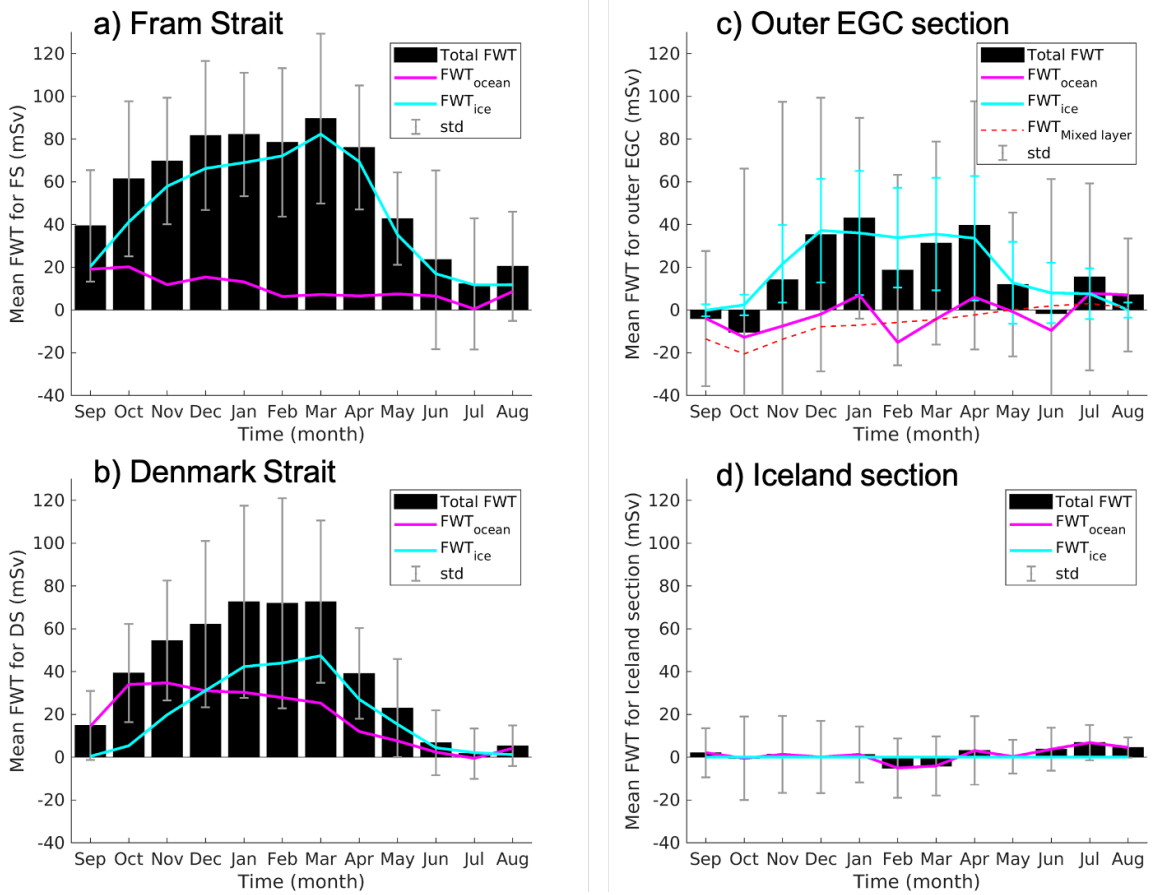


**Figure 8.** Mean seasonal cycles of simulated liquid freshwater transport (FWT<sub>ocean</sub>; magenta curves) and simulated solid freshwater transport (FWT<sub>ice</sub>; light blue curves) for the period 1973-2004. The total FWT is shown as black bars. The FWT is shown for all four sections in Fig. 1; a) Fram Strait, b) Denmark Strait, c) outer EGC section, and d) Iceland section. Positive FWT across Denmark Strait, outer EGC, and Iceland section means that the transport is out of the closed domain in Fig. 1. Note that the sign of the FWT across Fram Strait is reversed, i.e., positive FWT across Fram Strait means that the transport is into the closed domain. The standard deviation (std) of the detrended time series for the period 1973-2004 is added on the black bars (grey vertical lines). In c), the std is also shown for FWT<sub>ice</sub> (light blue vertical lines), and the red dashed curve shows the FWT in the mixed layer.

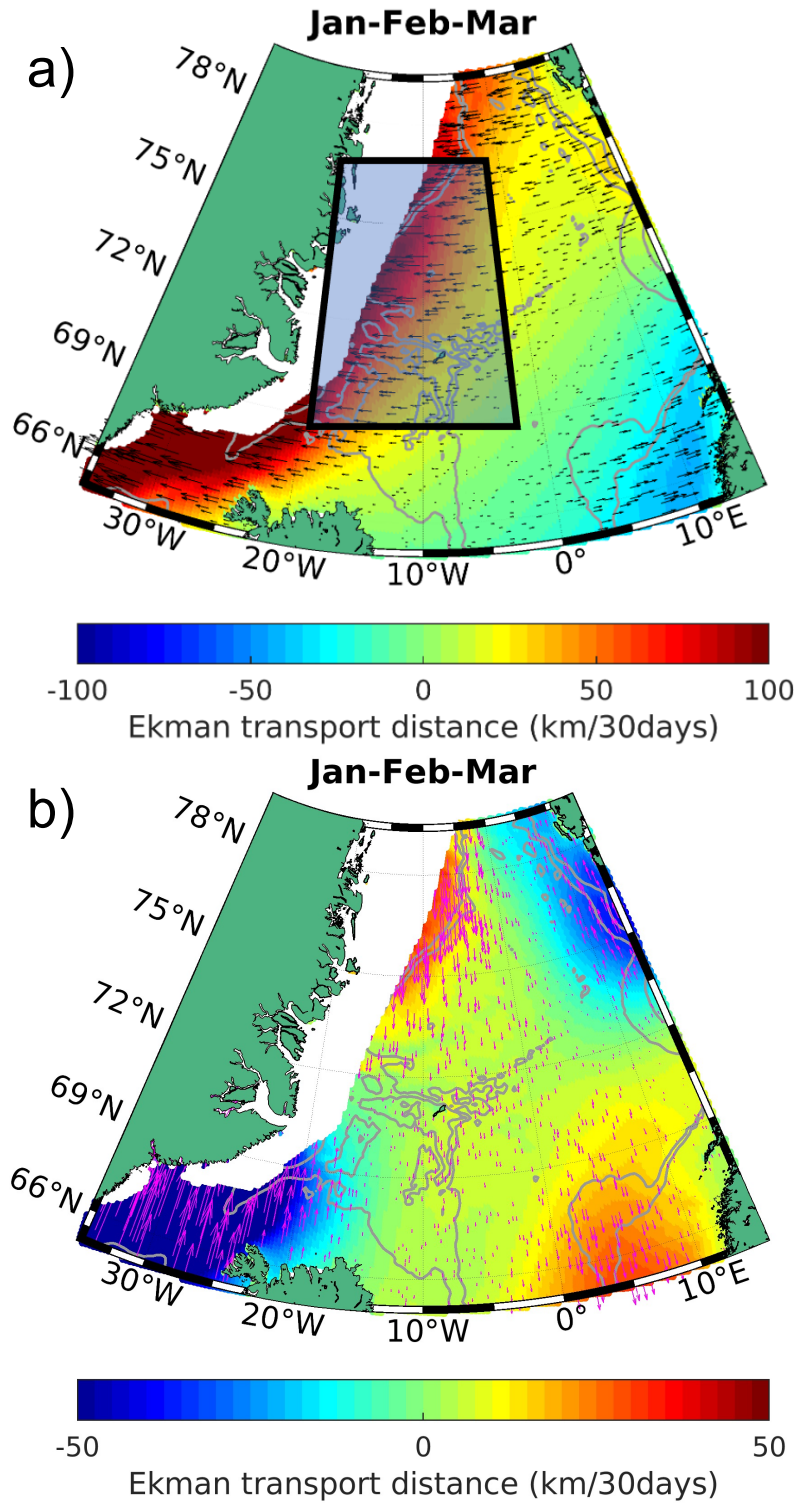


**Figure 9.** The simulated Ekman transport distance in winter for the period 1973-2004, where the magnitude is shown by colour. The direction of a) the zonal component (black) and b) the meridional component (magenta) of the Ekman transport is shown by the arrows. In the western Nordic Seas (defined by the box), the zonal component is westward and the meridional component is southward. The depth contours are 1200 and 2000m (thin grey lines). The white region is the area where the sea ice concentration is larger than 90%. Note the difference in the scale of the magnitude in a) and b).

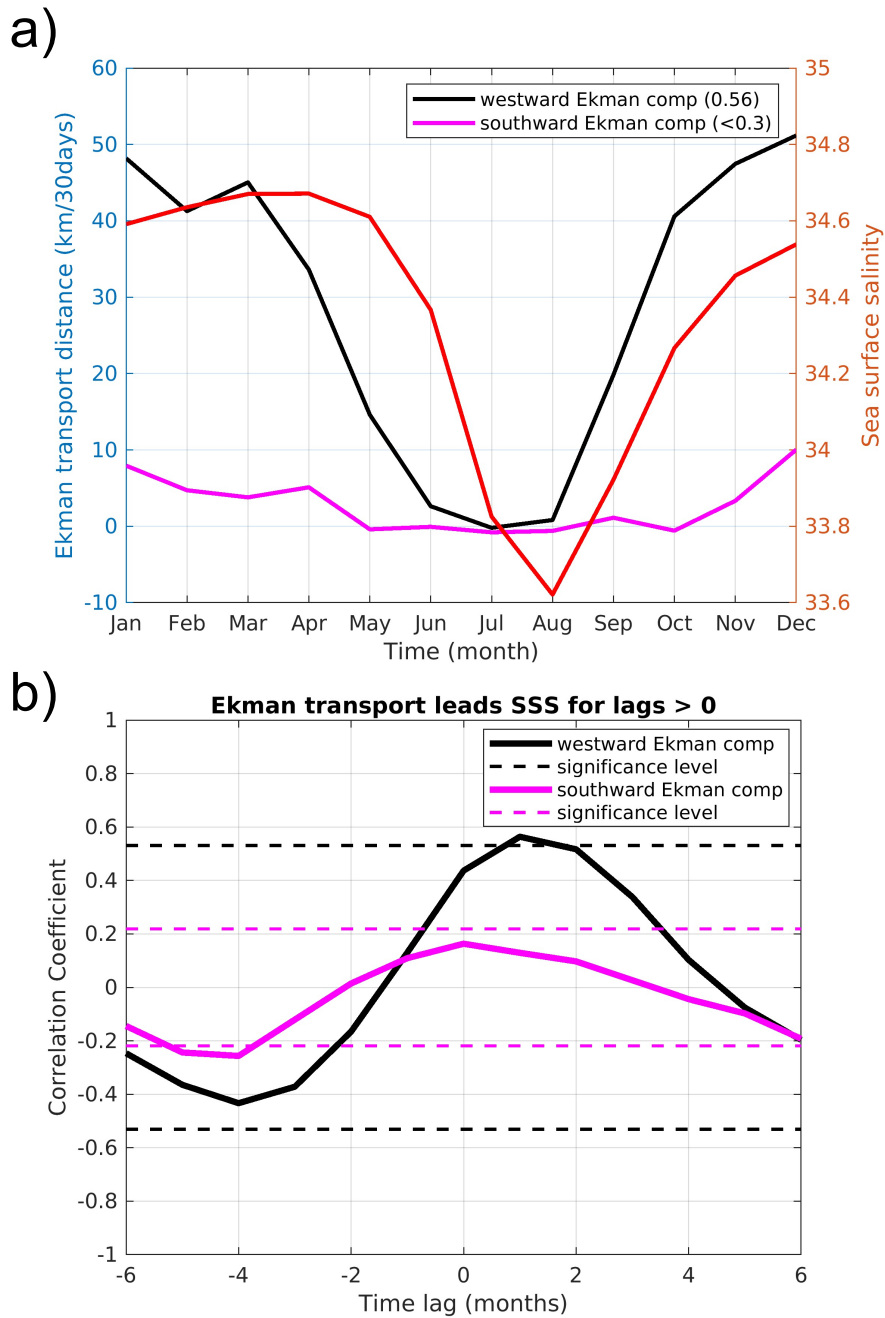


**Figure 10.** a) Mean seasonal cycles of simulated variables in the western Nordic Seas (averaged over the box domain in Fig. 9a). The scale for Ekman transport distance is shown on the left y-axis, whereas the scale for Sea Surface Salinity (SSS; red curve) is shown on the right y-axis. The numbers in parenthesis are the maximum correlation with SSS. b) Cross-correlation between SSS and Ekman transport distance (for each component separately), where we use all months for the full time period 1973-2004 (32\*12 points). The dashed lines mark the 95% significance level.

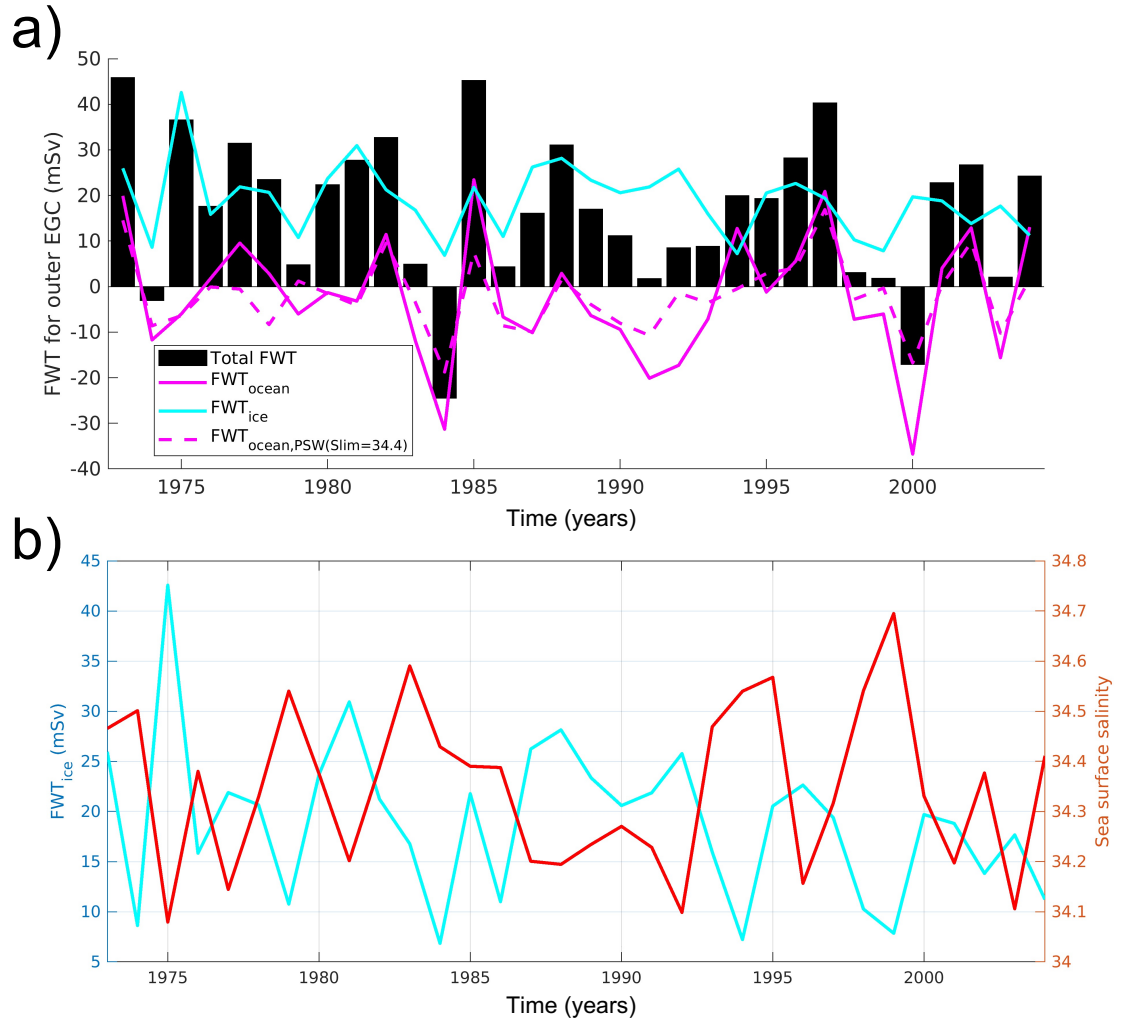


**Figure 11.** a) The annual mean total freshwater transport (FWT) across the outer EGC section in the model simulation. The liquid freshwater transport (FWT<sub>ocean</sub>) and solid freshwater transport (FWT<sub>ice</sub>) are also shown. The FWT<sub>ocean</sub> using a salinity limit of 34.4 is also shown (dashed line), in order to give an estimate of the liquid freshwater transport in Polar Surface Water (PSW). Positive values mean that the transport is out of the closed domain shown in Fig. 1. b) Temporal evolution of FWT<sub>ice</sub> and SSS in the western Nordic Seas (the latter is averaged over the box domain in Fig. 9a). The scale for FWT<sub>ice</sub> is shown on the left y-axis (blue), whereas the scale for SSS is shown on the right y-axis (red).

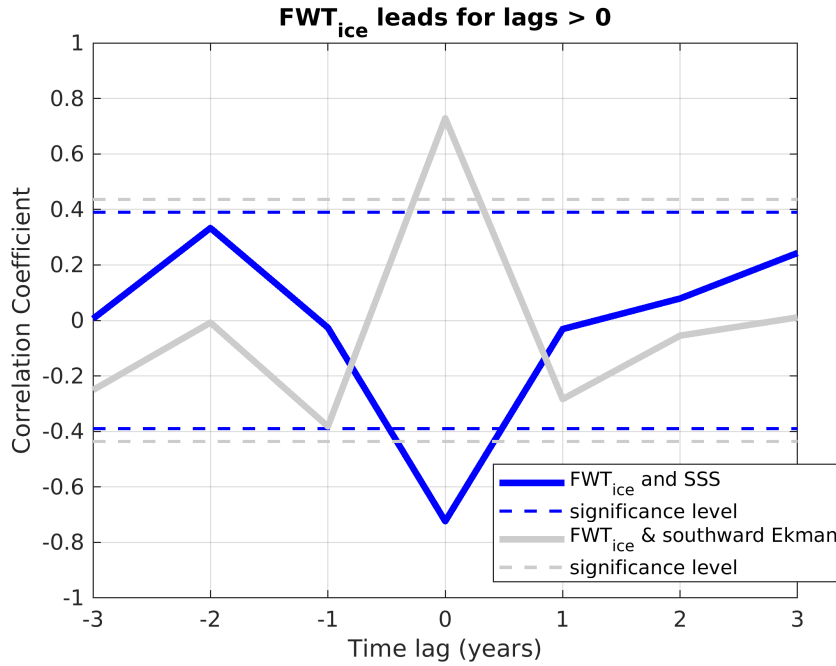


**Figure 12.** Cross-correlation between the solid freshwater transport ( $\text{FWT}_{\text{ice}}$ ) across the outer EGC section and SSS in the western Nordic Seas (blue curve), and cross-correlation between  $\text{FWT}_{\text{ice}}$  and the southward Ekman transport distance in the western Nordic Seas (gray curve). We use annual means for the period 1973-2004. The dashed lines mark the 95% significance level.

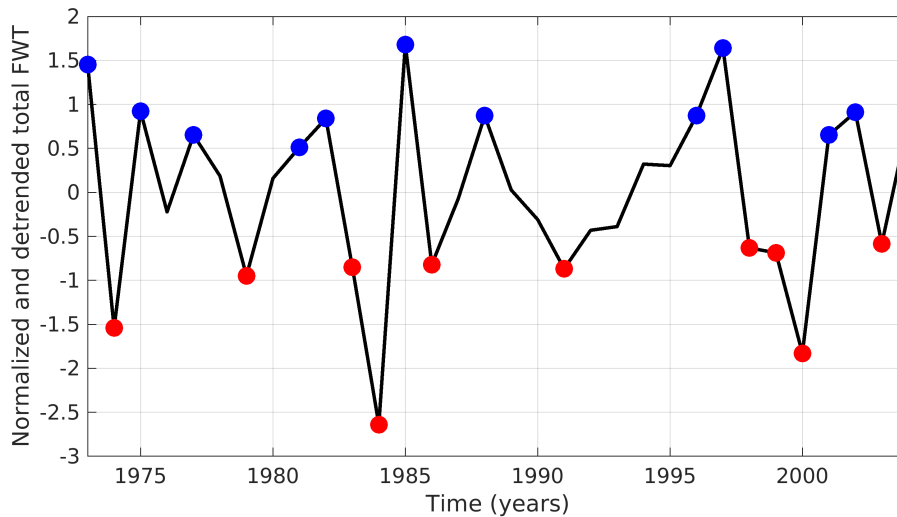


**Figure 13.** Time series of the normalized and detrended total freshwater transport (FWT) across the outer EGC section in the model simulation. Composite analysis is done for years with values above (below) the value 0.5, marked by blue (red) circles. The years with blue circles are those with high FWT into the interior of the Nordic Seas, and years with red circles are those with low FWT into the interior.

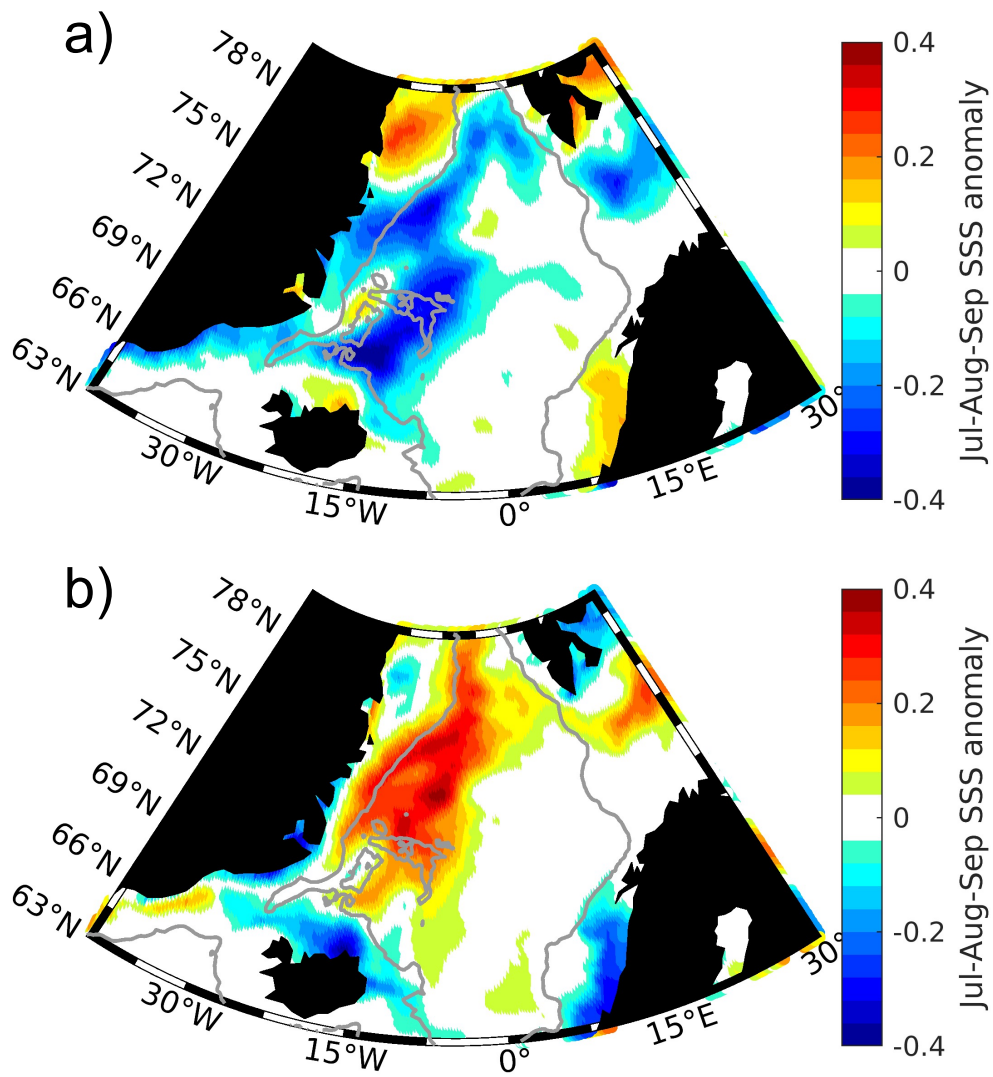


**Figure 14.** Composites of simulated SSS anomalies in late summer (Jul-Sep). a) and b) show anomalies associated with the years marked by blue and red circles, respectively, in Fig. 13. The thin grey lines show the 1200m isobath.